Chem Soc Rev

Visualizing the atherosclerotic plaque, a chemical perspective

Journal:	*Chemical Society Reviews*
Manuscript ID:	CS-TRV-11-2013-060410.R1
Article Type:	Review Article
Date Submitted by the Author:	24-Jan-2014
Complete List of Authors:	Garcia-Espana, Enrique; University of Valencia, Department of Inorganic Chemistry Albelda, M. Teresa; University of Valencia, Institute of Molecular Science Frias, Juan; Universidad CEU-Cardenal Herrera, Ciencias Biomedicas

Visualizing the atherosclerotic plaque, a chemical perspective

Mª Teresa Albelda,[†,§] Enrique Garcia-España[†] and Juan C. Frias*[,‡,§]

[†]*Universidad de Valencia, Instituto de Ciencia Molecular, Edificio de Institutos de Paterna, c/ Catedrático José Beltrán 2, 46071 Valencia, España*

[§]*GIBI230. Grupo de Investigación Biomédica en Imagen. IIS La Fe. Valencia*

[‡]*Universidad CEU-Cardenal Herrera, Departamento de Ciencias Biomédicas, Avda. Seminario s/n 46113 Moncada, Valencia, España*

Abstract

Atherosclerosis is the major underlying pathologic cause of coronary artery disease. An early detection of the disease can prevent clinical sequellae such as angina, myocardial infarction, and stroke. The different imaging techniques employed to visualize the atherosclerotic plaque provide information with diagnostic and prognostic value. Furthermore, the use of contrast agents helps to improve signal-to-noise ratio and provides better images although for certain imaging techniques (PET, SPECT) are absolutely necessary. We report on the different contrast agents that have been used, are used or may be used in future in animals, humans, or excised tissues for the distinct imaging modalities for atherosclerotic plaque imaging.

Introduction

Atherosclerosis is a chronic systemic disease that is characterized by hardening of the arteries through accumulation of lipids and fibrous elements to form atherosclerotic plaques. This process may be present as early as in the first decade (fatty streak), which is common in infants and young children,[1] and may progress to where the atheromatous plaque clinically manifests by blocking the lumen of the artery (ischemia) or ruptures to release the thrombogenic contents of its lipid core into the lumen with subsequent thrombus formation (thrombosis). Depending on the vascular territory affected, the clinical sequellae may be angina, myocardial infarction, stroke, or acute limb ischemia. In early atherogenesis, it is well known that lipoproteins accumulate in the subendothelial space of dysfunctional endothelium. This lipid material promotes the release of chemokines and increased endothelial cell expression of adhesion molecules, namely ICAM-1, VCAM-1 and P-selectin, which help recruit inflammatory leukocytes, especially monocyte-derived macrophages and T lymphocytes that are the key biomarkers and typically used for targeting the lesion for imaging.[2,3,4,5,6,7]

This complex disease process progresses from endothelial dysfunction to the formation of an atheromatous core. Proteins ($\alpha_v\beta_3$ integrin, matrix metalloproteinases (MMPs), VCAM-1, P-selectin, oxidized LDL, fibrin, collagen) and cells (endothelial, mast, resident macrophages, etc) that are critical in this process have been targeted using different molecular imaging probes.[8,9,10] Some of these imaging probes can also be utilized to identify myocardial damage and cardiac remodeling.[11,12,13] Over the past years, great advances have been made in

imaging techniques that enable visualization and characterization of atherosclerotic plaques at the cellular and molecular levels, as well as monitoring their progression or regression (Table 1).[14] The identification of atherosclerotic plaques by researchers has benefited from improvements in the different imaging techniques that are currently available. Among the most used for medical examinations of patients that could be at risk we find; magnetic resonance imaging (MRI), computed tomography (CT), positron emission tomography (PET), single photon emission computed tomography (SPECT), ultrasound (US), and optical imaging (OI).[15,16] An early detection of this chronic disease may direct therapies to prevent its complications.

Insert Table 1

Molecular imaging has been defined as the visualization, characterization, and noninvasive measurement of biological processes at the molecular and cellular levels in humans and other living systems spatially and temporally.[17] This discipline can help to identify the stage of disease, facilitate early diagnosis, offer fundamental information on pathological processes, and be applied to follow the efficacy of therapy. Molecular imaging may provide additional unique molecular and pathophysiological insight that will allow a more personalized approach to the evaluation and management of the cardiovascular disease. This application is based on the use of molecular probes or biomarkers to detect biological processes without disturbing their function.[18]

Imaging techniques can make use of contrast agents (CAs) to improve the quality of the images in the body by altering or enhancing tissues and thus, providing

contrast from other tissues. There are a large variety of elements that can be used as contrast agents for different imaging modalities. Metal ions play an important role in medicine and a large number of them are involved in the formulations of the different solutions employed for imaging studies. Non-metallic elements also serve an important role as imaging agents.[19] The variety of carriers utilized to deliver the contrast agents to the lesion is large; micelles, liposomes, dendrimers, polymers, modified proteins, lipoproteins, metallic nanoparticles, etc.[13,20]

It is complex from the chemical point of view to target the lesion because clinically approved contrast agents are non-specific for plaque imaging and it is complicated to clearly visualize the boundaries of the lesion in the vessels. Just in the case of gadofluorine M the agent targets the atherosclerotic plaque for imaging purposes without the presence of a homing moiety such a peptide or antibody to target any specific marker of the atheromata.

During the last years the term “theranostic” or “theragnostic” has strongly broken into literature. The term is a treatment strategy that combines therapeutic and diagnosis capabilities in a single agent. Although in cancer exists a large number of studies dealing with the theranostic concept, there are few examples of theranostic agents used to treat atherosclerotic lesions.[21]

Magnetic resonance imaging

Magnetic resonance imaging (MRI) is a noninvasive, nondestructive, 3-D imaging modality that makes use of the different relaxivity in water, fat, and other macromolecules within the body to produce an image. It has the advantage of providing very high spatial and temporal resolution along with excellent soft

tissue contrast for characterization of detailed cardiac anatomy and function. The main element for visualizing the plaques by MRI is hydrogen (H) and the characterization of atherosclerotic plaques without contrast agents is well documented.[22,23,24] However, contrast agents can be included in order to obtain better images. These substances provide larger contrast differences between the tissues based on differential distribution and can be classified whether they alter the longitudinal relaxation rate ($1/T_1$) more than the transverse relaxation rate ($1/T_2$) or *vice versa*. For contrast MRI, there are two main elements that are used with opposite features: gadolinium (Gd)[25] and iron (Fe).[26,27,28]

• Gadolinium

Gd is known as a positive contrast agent, since its dispensation increases the signal in the plaque due to an increase in $1/T_1$ and $1/T_2$ relaxation rates of nearby water molecules (Table 2).[29]

Insert Table 2

Since gadolinium ions are toxic, these must be chelated to reduce their toxicity. Two main chelating scaffolds are used to complex Gd^{3+} ions; an open lineal polyamine (diethylenetriamine) and a polyazamacrocyle (1,4,7,10-tetraazacyclododecane) both of them functionalized with carboxylic side arms to complete the coordination of the ion. Depending on the nature of the side arms there is a wide variety of contrast agents that have been used to visualize the atherosclerotic lesions. The following compounds shown in figures 1 and 2 have

been used to visualize the atherosclerotic plaque by MRI: Gd-DOTA, Gd-DTPA, Gd-DTPA-BMA, Gd-DO3A-butrol, Gd-HP-DO3A, Gd-BOPTA, Gd-Motexafin, MS-325, Gd-DTPA-BSA, Gd-DO3A-OA, Gd-DTPA-EB, Gd-DTPA-MPO, Gd-DOTAC16, Gd-DTPA-DMPE, Gadofluorine M, Gadomer 17, $Gd_3N@C_{80}$, B-22956/1, BMS753951, EP-2104R, P947, P792, Gd-DTPA-mimRGD, Gd-DTPA-g-R826, P717 and Gd-AAZTAC17.

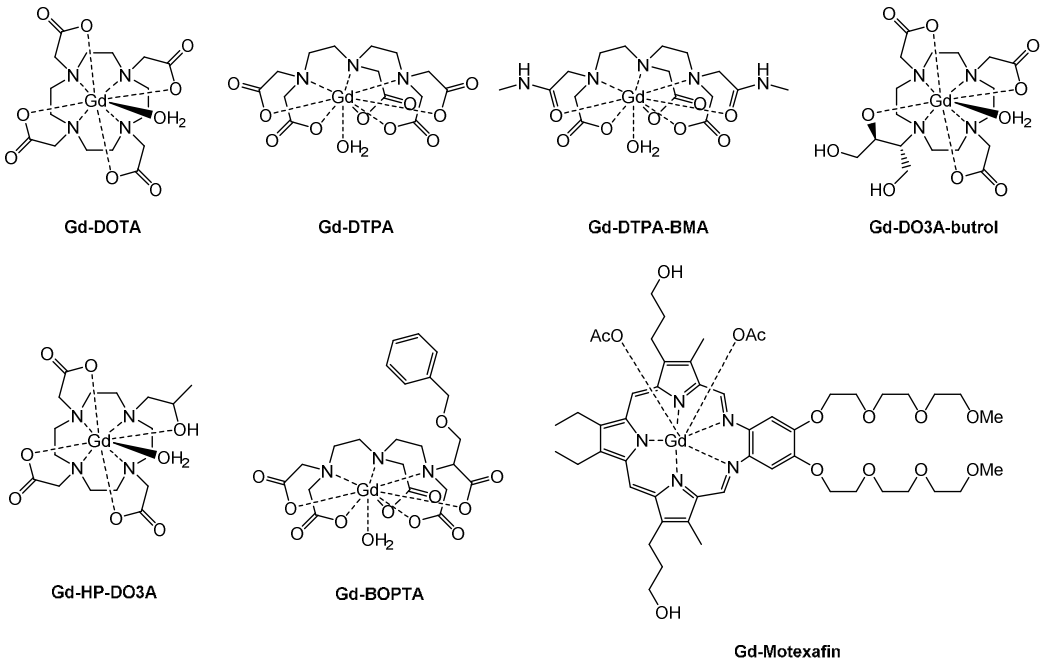

Figure 1. First generation of Gadolinium chelates for MRI.

Gd-DOTA (Fig. 1) revealed on carotid plaques that the enhancement obtained is associated with vulnerable plaque phenotypes and related to an inflammatory process.[30,31] Gd-DTPA (Fig. 1) has shown a strong association between intraplaque enhancement in severe intracranial atherosclerotic disease lesions and ischemic events with the use of conventional MR imaging.[32] By dynamic contrast-enhanced (DCE) MRI technique Gd-DTPA was used to image aortic or carotid plaques resulting in promising results that could be applied to monitor

high-risk patients and in longitudinal clinical drugs trials.[33,34] Using Gd-DTPA-BMA (Fig. 1) in combination with several 3D imaging sequences have provided enough contrast to distinguish necrotic core (NC), calcification (CA), loose matrix (LM).[35] Measures of plaque eccentricity are also associated with total cholesterol and non HDL-cholesterol in atherosclerotic plaques.[36] Gd-DO3A-butrol (Fig. 1) used in patients under chronic lipid apheresis therapy showed lower cholesterol, LDL and LDL/HDL when compared to a control group with similar degree of carotid stenosis.[37] Gd-HP-DO3A was compared with iodine for percutaneous intervention in atherosclerotic renal artery stenosis.[38] Gd-BOPTA (Fig. 1) was compared with Gd-DTPA-BMA. The authors found that the choice of the contrast agent has little impact on morphological characterization of carotid atherosclerotic plaque although DCE measurements showed differences.[39] Gd-Motexafin (Fig. 1) is an agent where the chelating moiety is derived from a pyrrole based ligand. This substance can generate contrast between various vascular tissue types and may be useful for plaque characterization of deep-seated arteries since is not quickly washout from blood stream.[40] This first generation of contrast agents are known to be extracellular. Thus the enhancement may be due to increased wash-in of gadolinium-based contrast agent, increased distribution volume and/or decrease washout.

A second generation of gadolinium contrast agents makes use of the chelating moieties and include features that allow incorporation to supramolecular aggregates (micelles, liposomes, lipoproteins); which increases the loading of gadolinium ions amplifying the signal, or contain molecules that recognize substances present in the atheromata (Fig. 2 and 3).

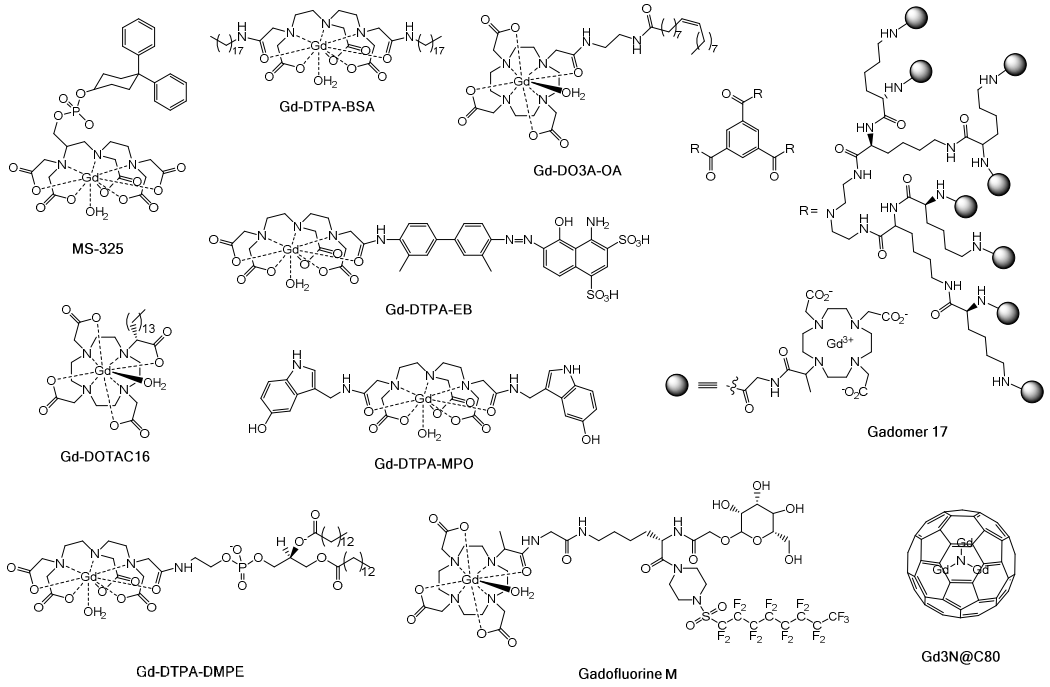

Figure 2. Second generation of Gadolinium chelates for MRI.

MS-325 (Fig. 2) was injected in patients with carotid artery stenosis for the detection of vulnerable plaque features. This contrast agent may add significant information to measurement of stenosis. Additionally, conjugation with contrast enhancement magnetic resonance angiography may help to stratify patients at risk and direct therapies to avoid complications.[41] The presence of two C_{18} aliphatic chains allows Gd-DTPA-BSA (Fig. 2) to be incorporated into lipoproteins[42] or liposomes.[43,44] These flexible supramolecular nanoagents can incorporate homing molecules such as antibodies,[45] proteins[46] or peptides[47] that target specific components into the atherosclerotic plaque. Following the previous design Gd-DO3A-OA (Fig. 2), a macrocycle that incorporates an aliphatic chain with a double bond was incorporated onto low-density lipoproteins (LDL). This gadolinium loaded LDL (>200 Gd^{3+} atoms per particle) led to discrete enhancement of aortic wall bearing atheroplaques.[48] Gd-DTPA-EB (Fig. 2) incorporates Evans blue dye that interacts with extracellular matrix and

vascular smooth cells of dysfunctional endothelium. The agent detected atherosclerotic plaques in the aorta and the T_1 signal intensity was increasingly enhanced with age.[49,50] Gd-DTPA-MPO (Fig. 2) is a contrast agent that achieves signal amplification by enzymatic addition instead of cleavage as previous enzyme-sensitive MRI agents were based. Gd-DTPA-MPO is highly sensitive and specific to myeloperoxidase activity.[51] In advanced human atherosclerotic vulnerable plaques, myeloperoxidase is expressed predominantly by activated macrophages and macrophage-derived foam cell. The agent demonstrated increased and prolonged contrast of atherosclerotic aortic wall, revealed areas of increased myeloperoxidase activity in atherosclerotic plaques and imaging results in more than a 2-fold increase in contrast in areas with increased myeloperoxidase activity.[52] Micelles and immunomicelles (macrophage scavenger receptor A, MSR-A antibody anti-CD204) of around 100 nm of diameter were prepared containing Gd-DOTAC16 (Fig. 2). Both preparations in *in vitro* and *ex vivo* experiments are superior MRI contrast agents compared to standard agents such as Gd-DTPA. Furthermore, immunomicelles enabled targeted macrophage MRI.[53] Gd-DTPA-DMPE (Fig. 2) is a phospholipidic agent where DTPA is bound to the phospholipids DMPE. This amphipatic agent was incorporated into the phospholipid surface of high-density lipoproteins (HDL).[54] Results show that the agent targets atherosclerotic lesions without the present of a homing molecule.[55] Gadofluorine M (Fig. 2) is a DOTA derived contrast agent that contains a perfluoroalkyl chain. Unlike aliphatic chains of Gd-DOTAC16, Gd-DTPA-BSA or Gd-DO3A-OA the fluorinated chain is not incorporated onto lipoproteins or liposomes but autoassemble in small size micelles (~ 6 nm). Gadofluorine M accumulates within the fibrous plaque or in the fibrous cap of a

plaque containing high amounts of extracellular matrix components but not in the lipid rich areas enabling detection of thin-cap fibroatheromas at multiple time points after injection widening the imaging window for assessing plaque stability.[56,57] Gadomer-17 (Fig. 2) is a dendritic macromolecular blood pool contrast agent with a DO3A moiety carries 24 Gd per molecule.[58,59] This agent improves coronary MR imaging and assessment of the coronary arteries in patients with substantial coronary artery disease.[60] Gd3N@C80 (Fig. 2) is a contrast agent where the gadolinium atoms are inside of a C_{80} fullerene.[61] This platform is further functionalized for intercalation within liposome bilayer membrane.[62] The resulting liposomes can incorporate antibodies for specific targeting. Conjugation with antibody CD36 provided enhanced visualization of foam cells present in the atherosclerotic lesions compared with non-targeted compounds that were not taken up either *in vitro* or *in vivo*.[63] B-22956/1 (Fig. 3) is a blood pool agent with a DTPA and deoxycholic acid moieties by means of a flexible spacer that binds with high affinity to serum albumin. At early time points injection of B-22956/1 produces enhancement of atherosclerotic plaques with MRI correlated with neovessel density and at later time points with macrophage density.[64] BMS753951 (Fig. 3) is an elastin-specific magnetic resonance contrast agent based on a functionalized DTPA. It has been used to demonstrate the feasibility of non-invasive assessment of progression and regression of plaque burden in a mouse model of accelerated atherosclerosis by quantifying changes in the content of elastin present in the extracellular matrix by signal intensity and T_1 measurements.[65] Fibrin is an important component of atherosclerotic plaque especially abundant in advanced lesions. EP-2104R (Fig. 3) is a gadolinium-based fibrin contrast agent that allows selective imaging and

quantification of intraplaque and endothelial fibrin.[66,67] Matrix metalloproteinases (MMPs) is a broad family of endopeptidases that are overexpressed in prone-to rupture atherosclerotic lesions as a consequence of inflammation and play a key role in the degradation and remodeling of the extracellular matrix. P947 (Fig. 3) is a DOTA derived agent with affinity for several MMPs that accumulates in atherosclerotic lesions.[68,69] P792 (Fig. 3) is a gadolinium blood-pool agent derived from DOTA that was used for aortic arch and carotid imaging.[70] Integrin $\alpha_v\beta_3$ mediates cell locomotion and migration through the extracellular matrix and seems to be a critical molecule for several processes involved in atherosclerosis progression and in restenosis. Gd-DTPA-mimRGD (Fig. 3) is a contrast that targets $\alpha_v\beta_3$ in vulnerable atherosclerotic plaques with a low washout compared to Gd-DTPA.[71] Gd-DTPA-g-R826 (Fig .3) is a DTPA derived agent that incorporates the peptide LIKKPF. This compound binds phosphatidylserine which is exposed on apoptotic macrophages within the lipid core in atherosclerotic plaques.[72] F-P717 and P717 (Fig. 3) are slow-clearance blood-pool macromolecular paramagnetic agents for targeting inflammation in vessel walls.[73,74] A new type of contrast agent based on a modified diazepine has been also employed to image the atherosclerotic plaque Gd-AAZTA-C17 (Fig. 3).[75,76]

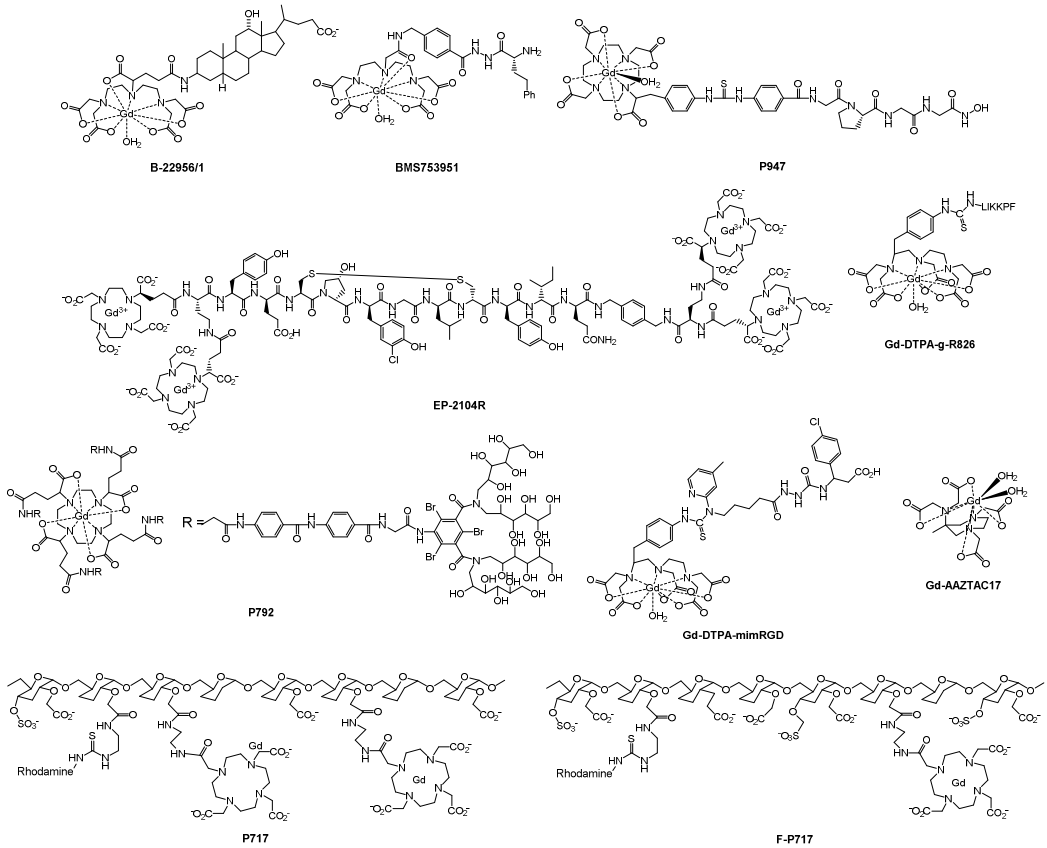

Figure 3. Second generation of Gadolinium chelates for MRI.

• Iron

In 1978, Ohgushi established that magnetic nanoparticles have the ability to shorten the T_2 relaxation times of water, and shortly thereafter, were used for magnetic resonance imaging.[77] Several types of iron oxide nanoparticles have been investigated for medical imaging applications.[78,79] Depending on their size we can classify iron oxide particles in: Ultrasmall superparamagnetic iron oxide (USPIO), with a diameter between 10 and 40 nm which has allowed detection of intraplaque macrophages of the aortic wall;[80,81] SPIO (superparamagnetic iron oxide) particles with an average size between 60 and 150 nm are internalized by macrophages present in the atherosclerotic plaques to an extent that can be detected by MRI;[82,83] and Microparticles of iron oxide (MPIO)[84] that have a mean diameter between 500 nm and 5 μm. There are two subcategories of USPIO

called monocrystalline iron oxide nanoparticles: MION[85] (with a diameter between 10 and 30 nm) and CLIO,[86] a form of MION with cross-linked dextran coating with a diameter around 10 and 30 nm. Iron nanoparticles are coated with different polymers to solubilize them such as dextran, carboxydextran, starch, PEG or as starting point for later functionalization with homing molecules or fluorescent probes. These nanoparticles have in common their specific uptake by the monocyte–macrophage system. Iron oxide is a negative contrast since its administration produces a darkening of the images in the plaque by a large increase in $1/T_2$.[87]

• Other elements

Both elements described above, gadolinium and iron, have found utility as MR contrast agents for *in vivo* imaging not only for animal models but also have been used for clinical diagnosis. Apart from them, however, there are some other elements that have been or are starting to be used for atherosclerosis detection. For instance, using fresh *ex vivo* human aortic samples with atheromata suspended in manganese chloride, Gold *et al*. were able to identify normal vessel wall components and other plaque components such as fibrous tissue, lipids, and possible areas of hemorrhage and hemosiderin deposition and correlated the MR characteristics with their histologic appearance.[88] Mn-DTPA has been included in the core of micelles for targeting oxidation-specific epitopes within the arterial wall.[89]

MRI of phosphorus (^{31}P) has been employed to observe calcification directly in *ex vivo* atherosclerotic plaques. Since calcification is composed of calcium phosphate and is the only source of crystalline ^{31}P in plaques this nucleus provides a fingerprint of calcification.[90]

A dysprosium diethylenetriaminepentaacetic acid hexamethylenediamine copolymer (Dy-DTPA polymer) (Fig. 4) a compound with a T_2 effect was employed to assess the arterial lumen size in areas of stenosis by black blood magnetic resonance angiography (MRA) in a rabbit model of atherosclerosis.[91]

Fluorine (^{19}F) is another element that is acquiring relevance in MRI since it is a nucleus that exhibits no background in the body compared with other nuclei that are omnipresent. ^{19}F permits absolute quantification of the concentration of tissue and it has unique spectral signatures. Perfluorocarbon-core nanoparticles are semipermeable agents able to reveal the presence of profound endothelial barrier disruption in later stage plaques.[92]

Hyperpolarized carbon-13 (^{13}C) molecules are gaining attention since background signal is extremely low because the natural abundance of ^{13}C is negligible. The long relaxation times (T_1 and T_2 up to ~60 and 5 s, respectively) make it possible to perform "real-time" vascular imaging with ^{13}C molecules to examine pathological conditions such as atherosclerosis.[93] Hyperpolarized TFPP (Fig. 4) is a compound that has shown to bind to the lipid content of atherosclerotic lesions in the aorta of LDLR-deficient mice.[94]

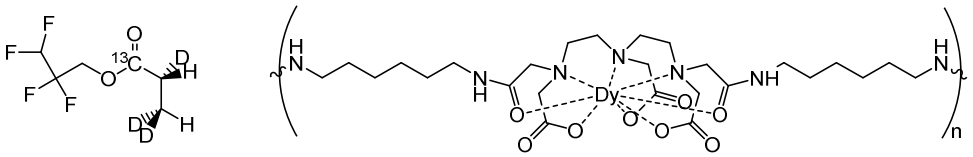

Figure 4. Hyperpolarized TFPP and a Dysprosium chelate for MRI of atherosclerosis.

Computed tomography

CT is a powerful anatomical imaging modality, which can be used for attenuation correction and adjustment of partial volume errors. CT technology has evolved from single image acquisition in minutes to obtaining multiple image slices in a single second with multidetector computed tomography scanners (MDCT) that provide submillimeter spatial resolution, allowing excellent visualization of the coronary arteries.[95] Due to the low electron-dense permeable soft tissues in the human body, unenhanced X-ray imaging cannot differentiate between different components of the atherosclerotic plaque. Therefore, appropriate electron-dense contrast agents that absorb light in the range of X-rays 10-0.01 nm corresponding to energies of 120 eV to 120 keV are required. To reach this goal several contrast agents mainly based on iodine substances, materials and even noble gases have been used in clinical procedures or experimental assays to visualize the atherosclerotic lesion.[96]

• Iodine

Iodine (I) is the principal element used for CT imaging contrast agents. There are a large number of agents (ionic, nonionic, dimers) that have been used to highlight the plaques.

Iodinated oil was formulated with quantum dots for dual imaging. The nanoemulsion specifically targeted macrophages and visualized atherosclerotic plaques by dual CT/fluorescence imaging.[97] Iodixanol (Fig. 5) is a dimeric nonionic agent that encapsulated into liposomes provides enough contrast from uptake of macrophages for atherosclerotic plaque imaging by a dual source micro-CT system.[98] Iohexol (Fig. 5), a monomeric nonionic compound, was encapsulated in immunoliposomes to target atherosclerotic plaques. This formulation is able to recognize inflammatory molecules (ICAM-1) and also to

deliver a high concentration of contrast agent for CT imaging.[99] Iomeprol (Fig. 5) a monomeric nonionic contrast agent has been used to locate atherosclerotic plaques in low-dose coronary CT angiography.[100,101] The monomeric nonionic agent iopamidol (Fig. 5) was used with FDG to assess high risk morphological features in plaques.[102] A monomeric nonionic iodine contrast agent, iopromide (Fig. 5) was employed for coronary artery calcium identification and quantification based on dual-energy coronary CT.[103] The iodine CT contrast agent ioversol (monomeric nonionic) (Fig. 5) was injected for a CT protocol of a triple rule-out coronary CT angiography that identifies noncoronary diagnoses limiting additional diagnostic testing to a low-to-moderate risk acute coronary syndrome (ACS) population.[104] N1177 (Fig. 5) a monomeric nonionic agent is uptaken by macrophages demonstrating a significantly increase enhancement in plaque two hours after injection (Fig. 5).[105]

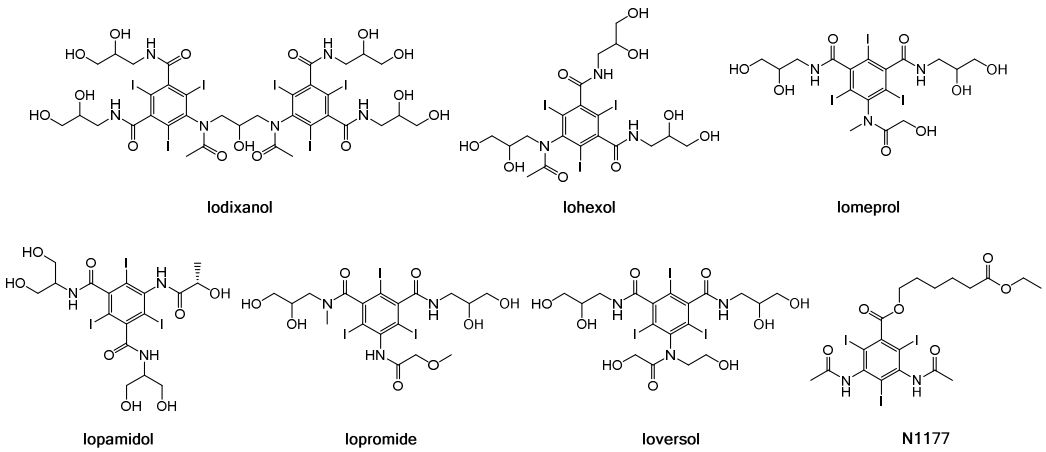

Figure 5. Iodinated compounds used as CT contrast agents.

• Other elements

Another element that is gaining more acceptance as a contrast agent for CT is gold (Au).[106] Gold, with its higher atomic number, has a higher X-ray absorption

coefficient than iodine. Imaging at 80-100 keV reduces interference from bone absorption and takes advantage of lower soft tissue absorption. In a murine model of atherosclerosis, the injection of a gold-based contrast agent showed signal enhancement in the aorta due to uptake of the contrast agent by macrophages present in the plaque.[107]

In the early 20th century, thorium (Th) was widely used as an X-ray contrast agent. Duff *et al.* demonstrated the uptake of colloidal thorium dioxide by atherosclerotic lesions in rabbits, although the aortas did not show shadows in roentgenograms when lesions infiltrated with the thorium contrast agent were exposed to X-rays.[108] This contrast was discarded since almost all systematically administrated ThO_2 was retained by the body and the toxicity arose from its radioactive isotope ^{232}Th, an α emitter.

In patients with contraindications for the use of iodine based contrast agents, such as azotemia or severe contrast allergy, gadolinium can be employed as an alternative. Gd has been used for carotid angiography in patients with suspected carotid stenosis showing a slightly inferior quality of images as compared with an iodine based contrast agent.[109]

A noble gas like xenon (Xe) with a high Z is the most commonly used for CT imaging. Xenon-CT has been used for several decades to evaluate cerebral blood flow and perfusion in patients with cerebrovascular disorders.[110,111,112]

PET and SPECT

Nuclear imaging techniques such as PET and SPECT make use of radionuclides and enable imaging of molecular interactions of biological processes including

inflammation and apoptosis.[113] Both techniques have sensitivities in the picomolar range but have the disadvantages of low spatial resolution and long acquisition time (Table 1), although rapid advances in technology are improving these drawbacks.[114] Additionally, the development of dual PET/CT, SPECT/CT, and PET/MRI machines makes possible the acquisition of morphological and molecular data with spatial co-registration in a single scanning session facilitating data interpretation and increased time efficiency.[115,116]

The variety of elements used for nuclear imaging of atherosclerotic lesions is quite large.[117,118,119] The radionuclides can be classified in two categories: non-metallic and metallic radioisotopes. Among the non-metallic radiotracers that have been utilized to image the atherosclerotic plaque we can cite tritium (^{3}H), carbon ($^{11/14}C$), fluorine (^{18}F) and iodine ($^{123/124/125/131}I$). Metallic tracers are mainly based on technetium (^{99m}Tc) and indium (^{111}In), although other elements such as copper (^{64}Cu), gallium (^{68}Ga), cobalt (^{55}Co), zirconium (^{89}Zr) can also be employed. Selection reasons of different elements for imaging purposes should be based on their half-life, energy, or the ease in varying the ligand for altering endogenous distribution of metal ions to the lesion (Table 3).

Insert Table 3

^{99m}Tc, which represents nearly 80% of all nuclear medicine procedures, and ^{111}In are the most commonly used isotopes in diagnostic nuclear medicine. Both tracers have been widely used in SPECT imaging of atherosclerotic lesions.[120,121]

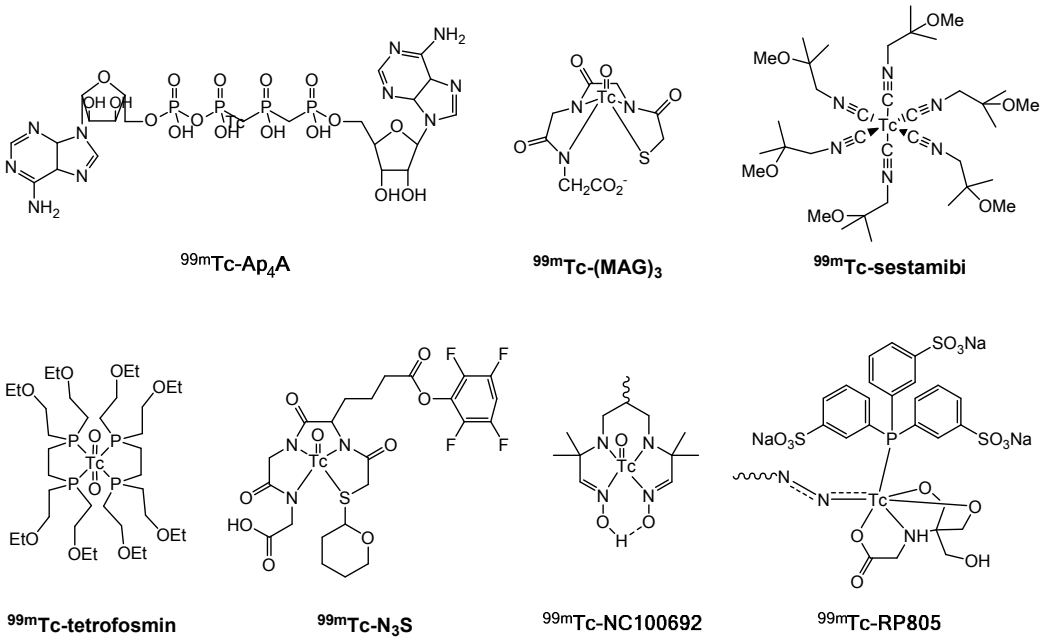

Figure 6. ^{99m}Tc chelates employed for atherosclerotic plaque imaging using SPECT technique.

• Technetium

^{99m}Tc is an excellent nuclide for developing molecular imaging radiopharmaceuticals for SPECT. Among the large variety of chelates that have been employed for atherosclerotic plaque imaging we can cite:

^{99m}Tc-Ap$_4$A (Fig. 6), this compound competes at ADP association sites on platelets making them potentially highly selective pharmacological agents for vascular lesions where platelets show early localization and aggregation.[122] ^{99m}Tc(CO)$_3$ was conjugated to annexin A5 that contains a fluorescent probe (AF568).[123] The uptake of the tracer increased in atherosclerotic carotid vasculature compared to control arteries.[124] ^{99m}Tc-HSA (human serum albumin) was used in a study with ^{111}In-tropolone labeled plateles for the study of a novel antiplatelet agent.[125] ^{99m}Tc-HYNIC has been conjugated to annexin V a protein with high affinity for phosphatidylserine an inner component of the plasma membrane that in apoptosis is exposed on the outer surface of smooth muscle

cells present in coronary atherosclerosis.[126] Since low-density lipoproteins are present in atheromata ^{99m}Tc-LDL was used to image the plaque although the background ratio obtained was not optimal since half-life of LDL in plasma ranges from 2 to 6 days while half-life of ^{99m}Tc is only 6 hours.[127] ^{99m}Tc-MAG_3 (Fig. 6) has been used to image atherosclerotic plaques at an early stage when is combined with antisense oligonucleotides.[128] ^{99m}Tc-sestamibi and ^{99m}Tc-tetrofosmin (Fig. 6) were used joint with CT imaging for assessing plaque extent and location.[129] ^{99m}Tc-N_3S (Fig. 6) has been coupled to interleukin-2 (IL2) for carotid plaque imaging since IL2 is a cytokine that acts by binding to its receptor (IL2R) expressed mainly on activated T lymphocytes.[130] ^{99m}Tc-NC100692 (Fig. 6) has been employed for carotid plaque imaging since NC100692 binds to $\alpha_v\beta_3$ integrin expressed by monocyte-derived macrophages.[131] Reduced pertechnetate ($^{99m}TcO_4^-$) binds to sulfhydryl groups on proteins. MDA2 is an antibody against murine malondialdehyde LDL (MDA-LDL) and specifically recognizes MDA-lysine epitopes. The ^{99m}Tc-MDA2 is accumulated in thoracic and abdominal aorta as determined by gamma imaging and also by pathological analysis.[132] ^{99m}TC-RP805 (Fig. 6) a MMP inhibitor compound has allowed molecular imaging detection of MMP activity in a wide spectrum of atherosclerotic lesion severities in transgenic mouse models.[133] ^{99m}Tc-ZK 167054 is an endothelin derivative utilized for atherosclerosis imaging due to the micro- to nanomolar affinity of ZK 167054 for endothelin-A and –B receptors implicated in the pathogenesis of atherosclerosis and restenosis.[134]

• Indium

A ^{111}In-DOTA (Fig. 7) derived tetrameric linear peptide (^{111}In-DOTA-TLP) that targets vascular cell adhesion molecule 1 (VCAM-1) has shown accumulation in

the root of excised aortas of apoE$^{-/-}$ mice.[135] ^{111}In-oxine (Fig. 7), a compound approved for human use was utilized to monitor and quantify early biodistribution in a murine model of progenitor cell therapy for atherosclerosis.[120] ^{111}In-RP782 is a tracer with specificity for activated MMPs. Since MMP activation plays a key role in vascular morbidity, mortality and is a key mediator of aneurysm expansion and rupture MMP-targeted imaging potentially may identify high-risk patients.[136] ^{111}In-SCN-Bz-DTPA (Fig. 7) was conjugated to LDL for plaque imaging. The results suggested that LDL is a good carrier but labeling with longer-lived radionuclides hold great promise.[137] ^{111}In-tropolone (Fig. 7) was used to label autologous platelets for deposition on active atherothrombotic lesions in order to study short-term E551 (an antiplatelet agent) therapy.[135]

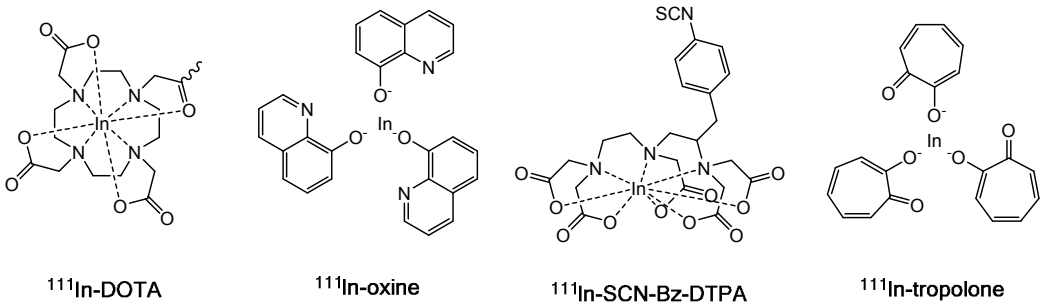

Figure 7. ^{111}In derivatives used as SPECT contrast agents.

• Fluor

For the development of PET radiopharmaceuticals, ^{18}F appears to be an ideal radionuclide due to several reasons; i) low positron energy, ii) it can be produced in high specific activity and large amounts, iii) it can react as an electrophile or a nucleophile, and iv) it has relatively high labeling yields.

^{18}F-EF5 (Fig. 8) is a specific marker of hypoxia labeled for PET in mouse

atherosclerosis plaques. The tracer showed uptake in large atherosclerotic plaques since these lesions contain hypoxic areas.[138] ^{18}F-AIF-NOTA-EBM (Fig. 8) is an elastin binding radiotracer. Elastin is considered a key player in human vascular diseases and it might contribute to the development of atherosclerosis. However no statistical significance was evident *in vitro* for accumulation in plaque samples compared to control samples of normal arteries.[139] ^{18}F-AppCHFppA (Fig. 8) has been used for quantifying the up-regulation of purine and specific oligonucleotide receptors in atherosclerotic lesions for noninvasive *in vivo* detection of plaque formation.[140] ^{18}F-FCH (Fig. 8) is a novel agent for imaging relevant aspects of plaque biology. Its colocalization with plaque macrophages may render it an additional marker of vascular inflammation suggesting vulnerability of an atherosclerotic plaque.[141] For atherosclerotic plaque imaging ^{18}F has been conjugated to glucose (^{18}F-FDG, Fig. 8) since this fluorodeoxyglucose is internalized by cells with a high metabolism (macrophages) and can distinguish between inflamed from non-inflamed plaque.[142] ^{18}F-galacto-RGD (Fig. 8) is a peptide tracer for PET imaging that binds with high specificity to $\alpha_v\beta_3$ integrin since its targeting imaging has been proposed as a strategy for detection of inflammation and angiogenesis in atherosclerotic lesions. ^{18}F-galacto-RGD showed focal, specific uptake in atherosclerotic plaques in the aorta of hypercholesterolemic mice. In this model uptake was highest in plaques with dense cell infiltrate composed mainly of macrophages.[143] ^{18}F-NaF has been used to measure active calcification of the coronary atherosclerosis *in vivo*.[144] 4-^{18}F-Fluorobenzoic acid (^{18}F-FBA, Fig. 8) was used to label LyP-1, a cyclic peptide which receptor is expressed in macrophages and foam cells present in atherosclerotic plaques.[145] ^{18}F-4V was

obtained from labeling peptide TLP with 4-^{18}F-fluorobenzaldehyde. ^{18}F-4V accumulates in atherosclerotic plaques due to detection of VCAM-1 expression.[139] Nowadays a new compound, ^{18}F-7 (Fig. 8), with inhibitory properties over MMP2/MMP9 is being tested for atherosclerosis imaging.[146]

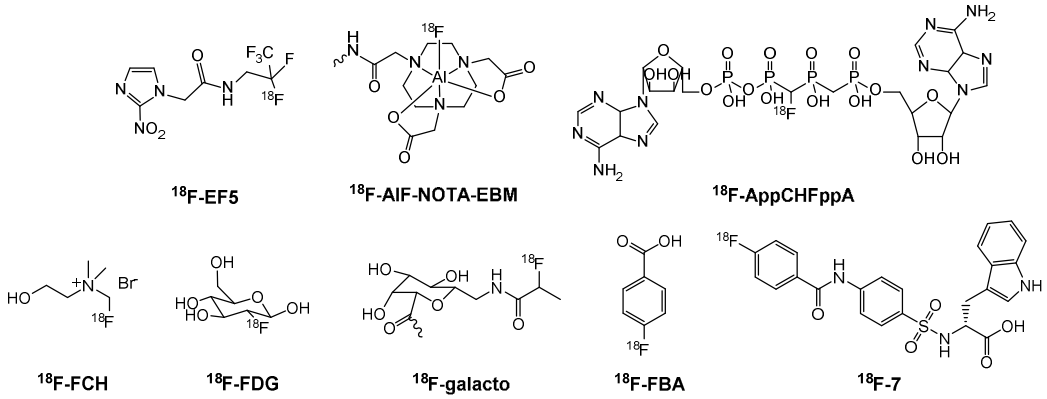

Figure 8. ^{18}F compounds used as PET radiopharmaceuticals.

• Iodine

There are four isotopes of iodine (^{123}I, ^{124}I, ^{125}I and ^{131}I) that have been utilized to image atherosclerotic lesions in animal models and humans.[147,148,149]

^{123}I-HO-CGS 27023A (Fig. 9) is a broad-spectrum MMP inhibitor for in vivo imaging of MMP activity. This radioligand was capable to image MMP activity in vivo in the MMP-rich vascular lesion developed in carotid artery of apoE-KO mice.[150] Interleukin 2 (IL2) was iodinated with Na^{123}I (1,3,4,6-tetrachloro-3,6-diphenylglycoluril, Iodo-Gen) to produce ^{123}I-IL2. The purpose of the study was to identify inflamed plaques in a high-risk group of patients.[151] ^{123}I-LDL was iodinated with Na^{123}I and injected to patients for scintigraphic studies. Patients showed accumulation in certain vascular areas with lipid entry ratio.[152] SP4 is a oligopeptide fragment of apolipoprotein B that has demonstrated pronounced uptake in the healing edges of balloon-injured rabbit aortic endothelium. SP4

was iodinated, ^{123}I-SP4, for identification of atherosclerotic plaques. The results revealed that ^{123}I-SP4 localize specifically in the aortic atherosclerotic lesion.[153] ^{124}I was introduced in antibody CD68 where plays a key role in atherosclerotic lesion formation. Imaging of ^{124}I-CD68 correlated well with plaque extension when compared with histopathological studies of the aortic arch.[154] Hypericin a natural photodynamic pigment was labeled with ^{124}I (^{124}I-Hypericin, Fig. 9) for PET imaging of apoptosis and necrosis in atherosclerosis. The radiotracer is uptaken in the lesion and was able to target necrosis.[124]

Cholesteryl ipanoate was radiolabeled with ^{125}I via an iodine exchange reaction in a pivalic acid melt. ^{125}I-CI was transported to the lesion by acetylated LDL (acLDL) and resulted in selective uptake and retention at the site of early atherosclerotic lesion.[155] Cholesteryl 1,3-diiopanoate glyceryl ether (C2I) was labeled with ^{125}I via an iodine-exchange reaction. Results from animal studies demonstrated selective uptake and retention of radiolabeled C2I in rabbit atherosclerotic lesions when ^{125}I-C2I (Fig. 9) was carried via acLDL.[156] Platelet glycoprotein VI (GPVI) has been identified as the major platelet collagen receptor in vivo. ^{125}I-GPVI was obtained via ^{125}I iodination Iodo-Gen. *In vivo* and *ex vivo* imaging revealed substantial accumulation of ^{125}I-GPVI in the injured artery wall.[157] ^{125}I-IK17 is a human autoantibody iodinated with Enzymobeads that localizes to atherosclerotic lesions of LDLR$^{-/-}$ mice, suggesting that it specifically binds to oxidation-specific epitopes in the lesions.[158] LDL was radiolabeled with ^{125}I by use of the iodine monochloride method. ^{125}I-LDL accumulated in human atherosclerotic plaque and this accumulation by macrophages provides strong support to the hypothesis that these cells play a crucial role in the pathogenesis of atherosclerosis.[159] L19 is a specific antibody against extra-domain B (ED-B) of

fibronectin a marker of tissue remodeling and angiogenesis. L19 was labeled with $Na^{125}I$ (Iodo-Gen) to afford ^{125}I-L19 that is able to selectively target atherosclerotic plaques in apoE$^{-/-}$ mice.[147] ^{125}I-MDA2 an oxidation-specific antibody to malondialdehyde LDL (MDA-LDL) produced by iodination with $Na^{125}I$ showed aortic uptake reflects changes in plaque composition that are consistent with established features plaque stabilization, such as enhanced collagen and SMC content.[160] ^{125}I-SIB (Fig. 9) was conjugated with a peptide that binds to oxidized LDL (oxLDL) to afford ^{125}I-AHP7. This radiocompound showed selective and specific binding to oxLDL in atherosclerotic plaques mirroring oxLDL distribution.[161] ^{125}I-SP4 was obtained according to the adaption of the chloramine-T method. The radiotracer specifically localizes in aortic atherosclerotic plaques in cholesterol fed rabbits.[162]

^{131}I-LDL was obtained by iodination of LDL with iodine monochloride and $Na^{131}I$. The compound accumulated in treated patients with confirmed atherosclerotic lesions (Fig. 9).[147]

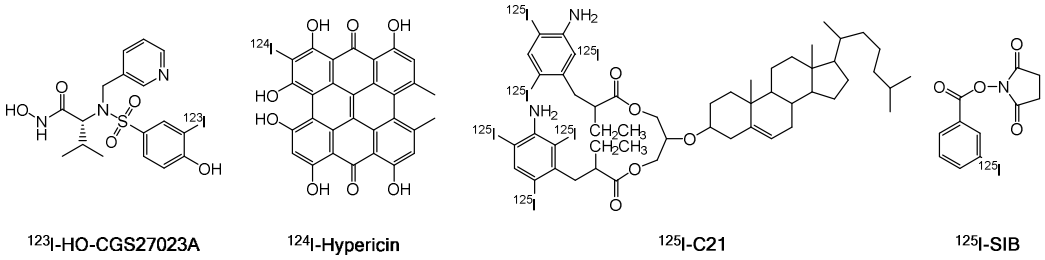

Figure 9. Iodinated radioligands.

• Gallium

In atherosclerosis imaging ^{68}Ga-DOTA (Fig. 10) derivatives such as ^{68}Ga-DOTA-TATE,[163] ^{68}Ga-DOTA-TOC[164] and ^{68}Ga-DOTA-RGD[165] have showed clear plaque

uptake in atherosclerotic plaques. The uptake has shown strong association with known risk factors of cardiovascular disease.

• Copper

A tracer for PET imaging that avoids the rapid radioactive decay of ^{18}F is ^{64}Cu. ^{18}F in a modified sugar targets areas of high metabolic rate, which may not necessarily represent the enhanced metabolic activity seen with inflammatory cells. ^{64}Cu-DOTA (Fig. 10) derivatives show uptake at the site of atherosclerosis.[166,167] ^{64}Cu-DTPA (Fig. 10) provides a different means of identifying atherosclerosis by accumulating in regions of mouse atheroma where phagocytic cells uptake the tracer.[168]

• Zirconium

^{89}Zr-DNP (dextran nanoparticles) were obtained by mixing cross-linked dextran and ^{89}Zr-SCN-Bz-Df (p-isothiocyanatobenzyl desferoxamine, Fig. 10). The nanoparticles were injected in atherosclerotic animals revealing that the majority of the signal derived from macrophages in the atherosclerotic plaques.[169] Bevacizumab conjugation and labeling with ^{89}Zr was achieved by succinylate desferal (^{89}Zr-sucDf). The tracer targets intraplaque released vascular endothelial growth factor (VEGF) that is known to be an important process linked to plaque vulnerability (Fig. 10).[170]

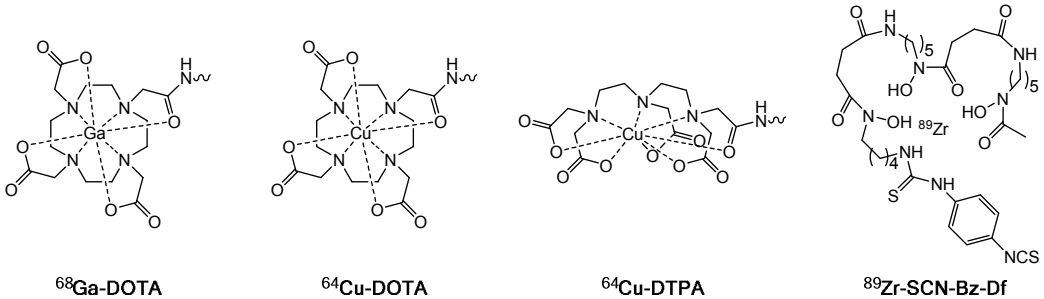

Figure 10. PET radiotracers for atherosclerosis imaging.

• Carbon

^{11}C offers the greatest potential to develop radiotracers for routine clinical applications because ^{11}C, as a label, can be easily substituted for a stable carbon in an organic compound without changing the biochemical and pharmacological properties of the molecule. Furthermore, the short half-life of ^{11}C provides favorable radiation dosimetry to perform multiple studies in the same subject under different conditions.[171]

^{11}C-acetate (Fig. 11) has been used for imaging of fatty acid synthesis in the atherosclerotic vessel wall.[172] ^{11}C-choline (Fig. 11) for visualizing the synthesis of phospholipids is a promising marker of plaque inflammation with potential advantages over ^{18}F-FDG. Elevated uptake of ^{11}C-choline was found in the carotid arteries and rarely correspond to calcification sites.[173] ^{11}C-PK11195 (Fig. 11) is a selective ligand of the translocator protein (TSPO) which is highly expressed by activated macrophages. Imaging intraplaque inflammation *in vivo* with ^{11}C-PK11195 can distinguish between recently symptomatic and asymptomatic plaques.[174]

^{14}C-antipyrine (Fig. 11) a metabolically inert diffusible indicator was evaluated for tracer distribution across the thoracic and abdominal aortas.[175] ^{14}C-FDG (Fig. 11) was used to compare uptake of ^{18}F-FCH.[141]

• Tritium

^{3}H-DAA1106 (Fig. 11) binds to atherosclerotic plaques with same topography as ^{3}H-PK11195 (Fig. 11). Both tracers had statistically significant topographical co-incidence within each plaque which was largely restricted to the shoulder and

cap regions a macrophage rich area.[176]

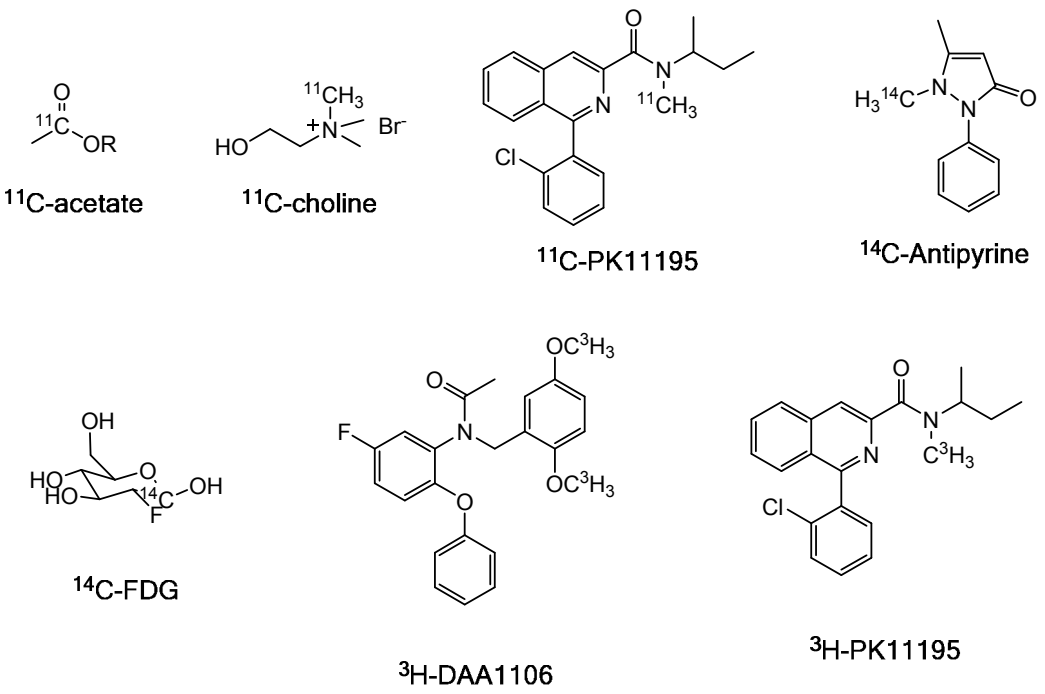

Figure 11. PET radiotracers for atherosclerosis imaging.

Ultrasound

US is the most widely used imaging technique in the world. It is a versatile, noninvasive, low risk, low cost, and portable real-time imaging technique. US CAs are typically gas micrometer size bubbles, encapsulated by a protein, polymer, or lipid shell. The rationale for using microbubbles as an ultrasound contrast agent is based primarily on their compressibility. Because they are gas filled and smaller than the diagnostic ultrasound's wavelength, microbubbles undergo volumetric oscillation in an acoustic field, such that they compress during the pressure peaks and expand during the pressure nadirs.[177,178]

Few elements are employed as contrast agents for US imaging. The micro-size bubbles have been filled with low molecular weight perfluorocarbons (C_nF_{2n+2}, n

= 3, 4),[179,180] SF_6,[181] N_2[182] or air (Fig. 12).[183]

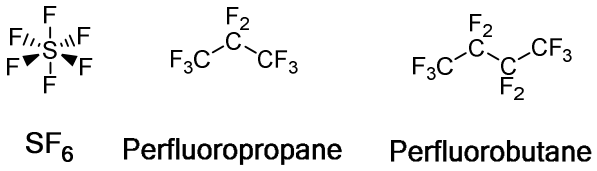

Figure 12. Ultrasound contrast agents.

Optical imaging

OI techniques offer several advantages such as high sensitivity, spatial resolution, non-ionizing radiation, and uses relatively simple instrumentation. It also enables rapid acquisition of images and is relatively inexpensive. There are several optical imaging techniques such as fluorescence and bioluminescence imaging, which can be used to non-invasively visualize biological processes.[184,185] These fluorescent probes are a moiety of a whole multifunctional contrast agent. There are a wide variety of chromophores that are used to visualize the atherosclerotic lesion. Near infrared fluorescent (NIRF) dyes are based on organic molecules with common elements (C, H, N, O, and S) where an aliphatic conjugated chain of an odd number of carbons (polymethines) is linked to two nitrogens of an aromatic system, benzoindolic or indolic, which determines the excitation and fluorescence emission wavelength range. These dyes have been used to image *ex vivo* and *in vivo* atherosclerotic lesions by reporting metabolic processes present in the plaque. Among them we can cite cyanine dyes such as Cy5.5 (Fig. 13),[186] Cy7 (Fig. 13),[143] VivoTag,[187] AngioSPARK,[188] NIR-664,[189] FITC (Fig. 13),[190] Photofrin II (Fig. 13),[191] Alexa Fluor 568 (AF568, Fig. 13),[124] DiO and DiI (Fig. 13).[192] Quantum dots (Qdots) are another type of contrast agents

employed to image atherosclerotic lesions.[193]

An expanded porphyrin (texaphyrin) chelate to lutetium (Lu-motexafin, Fig. 13)[194,]has been used for photoangioplasty of the atheromatous plaque and a DOTA derivative (Eu-P947, Fig. 13)[195] have been employed recently to detect unstable atherosclerosis due to its accumulation in the fibrous cap region of plaques.

Gold nanoparticles (AuNPs), with their biocompatibility, high optical scattering coefficients, and the fact that the optical spectra can be tuned by changing the size and/or shape of the particles, have been used to image atherosclerotic plaques *ex vivo* in rabbit aorta by intravascular photoacoustic (IVPA) imaging.[196]

Rhodamine (Fig. 13),[197] blue nile (Fig. 13),[198] hypericin[124] and NBD (Fig. 13)[55] dyes have been utilized in liposomes preparations for plaque imaging co-localization.

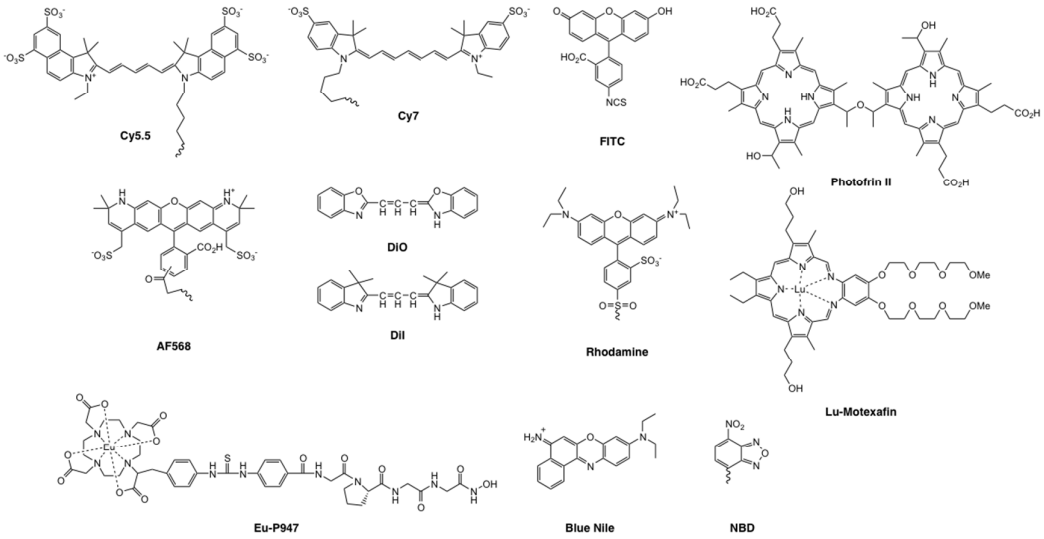

Figure 13. Contrast agents for optical imaging.

Hybrid contrast agents

Hybrid imaging techniques are of increasing relevance in the field of molecular imaging. The clinical machines that bring together imaging techniques such as PET/MRI, PET/CT, SPECT/CT, MRI/OI or experimental equipment such as FMT/CT (fluorescence microscopy tomography, FMT) just reveal the necessity of new contrast agents that join in a single molecule or nanoscaffold the distinct atoms necessary to produce the contrast for the different imaging modalities. At this respect there is a large number of studies of MRI/OI where the platform; usually a liposome, micelle, or iron oxide nanoparticle, incorporates a fluorescent probe. Although scarce, contrast agents that are suitable for FMT/CT,[187] SPECT/CT,[199] PET/MRI,[167] PET/CT,[168] CT/MRI,[107] PET or SPECT/OI[200] and a PET/MRI/OI[168] can be found in the literature.

Practical Considerations from a Chemical Perspective

As it has been exposed above, there are a high variety of extracellular contrast agents for the different imaging technologies that have been used for atherosclerotic plaque imaging. Single molecules are difficult to target the lesion without any help from homing moieties despite the fact of a dysfunctional endothelium that facilitates the permeability from the vessels. Just in few cases the contrast agents were capable to target the lesion. For the rest of contrast agents presented targeting to the atheromata is achieved by anchoring the agent to a vehicle that incorporates a targeting moiety or direct attach to an antibody. The use of nanoscaffolds produces an amplification of the signal and the possibility to incorporate contrast agents for different imaging technologies.

For MRI, in particular gadolinium agents, there is still improvement capacity of

the relaxivity for high and ultrahigh magnetic field strengths (3–16.4 T) since the efficacy of targeted and responsive contrast agents still depends on this.[201] Iodine plays a major role in CT imaging since practically all contrast agents employed are based on this element. However, gold nanoparticles and are becoming an alternative as they are easily produced and have higher absorption coefficientsMetal-based radioagents has made great strides in radioisotope coordination, production and their behavior *in vivo*.[202,203] The major drawback concerning radioelements is that some unpredictable supply shortages are becoming a perennial cycling and a growing threat due to their production in different accelerators or reactors. Fluorine and sulfur as different gas compounds are mainly used as ultrasound contrast agents. The carriers that entrap the gas are based on proteins, polymers or phospholipids that can be functionalized for specific targeting.[204] Finally, optical agents can be cataloged in three main groups: organic, inorganic or hybrid in nature.[205] Optical agents are usually a moiety added to help to characterize the lesion but due to the high sensitivity of fluorescence techniques they are becoming an independent way to assess atherosclerotic lesions.

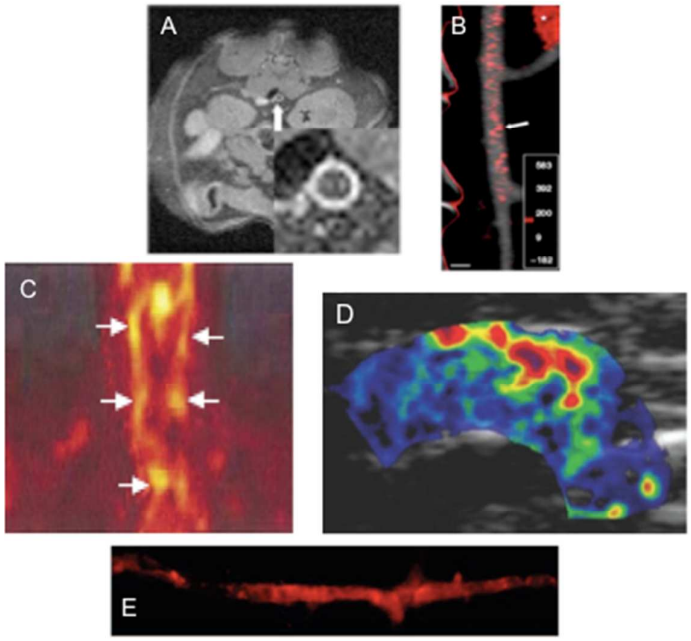

Figure 14. (A) MRI of atherosclerotic lesion with Gd. Arrow points the abdominal aorta, inset denotes magnification [Reproduced from ref 55 with permission]. (B) CT of atherosclerotic plaques in aorta with I. The white arrows point to red spots where atherosclerotic plaques were detected [Reproduced from ref 105 with permission]. (C) PET imaging with ^{18}F of carotid and aortic arch arteries [Reproduced from ref 142 with permission]. (D) Ultrasound targeted microbubbles in aortic arch for early stages of intimal xanthoma [Reproduced from ref 178 with permission]. (E) Fluorescence image of aorta injected with Qdots. The red color is due to the presence of plaques [Reproduced from ref 13 with permission].

Conclusion

Nowadays, atherosclerosis can be detected by a variety of imaging technologies at a cellular and molecular level. Progress has made possible the presence of dual machines PET/CT, SPECT/CT, PET/MRI, and more recently FMT/CT and IVPA, where different imaging modalities exist facilitating the acquisition of data. In a near future, advances in technology will improve detection limits and image quality of the techniques allowing to obtain images with lower doses of contrast agents. Also, new elements of the periodic table are employed as CAs. F and C can

be good candidates for MR imaging since previous assays have shown that both elements have no background signal within the body resulting in clear images. Au and Bi^{206} have already been used as CAs for CT and also for IVPA. The choice of the right element joint with the carrier and the ligand in the case of metal ions, and imaging technology can favor to obtain quality images of the atherosclerotic lesion.

Acknowledgments

The authors thank funds from Fundación Gent per Gent, Project CONSOLIDER INGENIO CSD-2010-00065 and Project PROMETEO 2011/008.

Table 1 Summary of imaging modalities

Imaging technique	Spatial resolution	Depth	Sensitivity	Acquisition Time	Radiation used in imaging generation	Cost
MRI	10-100 μm	No limit	nmol (10^{-9})	min/h	radiowaves	High
CT	50-200 μm	No limit	μmol (10^{-6})	min	X-rays	Medium
PET	1-2 mm	No limit	fmol (10^{-15})	s/h	high-energy γ rays	High
SPECT	1-2 mm	No limit	fmol (10^{-14})	min/h	low-energy γ rays	Medium
US	50-500 μm	mm to cm	nmol (10^{-8})	s/min	high-frequency sound	Medium
OI	1-5 mm	<1-2 mm	pmol (10^{-12})	s/min	Vis-NIR light	Low-medium

Table 2 Relaxivity of the gadolinium complexes used for atherosclerotic plaque imaging

Compound	r_1 ($mM^{-1}s^{-1}$)	^1H freq (MHz)	Temp (°C)	Ref
Gd-DOTA	3.56	20	39	25
Gd-DTPA	3.8	20	25	25
Gd-DTPA-BMA	3.96	20	35	25
Gd-DO3A-butrol	3,6	40	40	25
Gd-HP-DO3A	3.7	20	40	25
Gd-BOPTA	5.2	20	25	25
Gd-Motexafin	5.3	50	25	25
MS-325	6.6	20	37	25
Gd-DTPA-BSA	7.8	60	40	44
Gd-DO3A-OA	20.2	60	25	47
Gd-DTPA-EB	4.9	60	37	50
Gd-DTPA-MPO	4.3	20	40	51
Gd-$DOTAC_{16}$	37.3	60	25	53
Gd-DTPA-DMPE	12	20	25	54
Gadofluorine M	17.5	60	37	57
Gadomer-17	17.3	20	39	25
$Gd_3N@C_{80}$	20	400	30	61
B-22956/1	27	60	39 (h.s.)	64
BMS753951	4.68	128		65
EP-2104R	11.1	20	37	67
P947	5.5	60	37	68
P792	39	20	37	70
Gd-DTPA-mimRGD	4.3	60	37	70
Gd-DTPA-g-R826	9,6	20		
P717	9.41	60		72
F-P717	11.7	60		73
Gd-AAZTA-C_{17}	25	20	37	74

Table 3 Radionuclides used in PET and SPECT imaging for atherosclerosis

	Radionuclides	$t_{1/2}$	Decay	Energy[a] (keV)		
				E_{β^+}	E_{β^-}	E_{γ}
PET	^{11}C	20.38 min	β^+	386		511
	^{68}Ga	67.71 min	EC, β^+	836		511
	^{18}F	109.77 min	EC, β^+	250		511
	^{64}Cu	12.70 h	EC, β^+, β^-	278	191	511
	^{89}Zr	78.41 h	EC, β^+	395		
	^{124}I	4.18 d	EC, β^+	687		603
	^{3}H	12.32 y	β^-		5.7	
	^{14}C	5700 y	β^-		49.5	
SPECT	^{99m}Tc	6.01 h	IT, β^-			140
	^{123}I	13.22 h	EC, β^+			159
	^{111}In	2.80 d	EC			245
	^{131}I	8.02 d	β^-		606	364
	^{125}I	59.40 d	EC			27

min, minutes; h, hours; d, days; y, years

EC, electron capture; IT, isomeric transition; β^+, positron decay; β^-, beta decay

[a] National Nuclear Data Center, information extracted from the NuDat 2 database, http://www.nndc.bnl.gov/nudat2/.

References

[1] H. C. Stary, Am. J. Clin. Nutr., 2000, **72** *(Suppl. 5),* 1297S-1306S.

[2] P. Libby, *Nature,* 2002, **420**, 868-874.

[3] G. K. Hansson, *N. Engl. J. Med.,* 2005, **352**, 1685-1695.

[4] C. K. Glass and J. L. Witztum, *Cell,* 2001, **104**, 503-516.

[5] P. Libby, P. M. Ridker and G. K. Hansson, *Nature,* 2011, **473**, 317-325.

[6] A. J. Lusis, *Nature*, 2000, **407**, 233-241.

[7] R. Ross, *N. Engl. J. Med*., 1999, **340**, 115-126.

[8] S. Y. Shaw, *Nat. Rev. Cardiol.,* 2009, **6**, 569-579.

[9] M. J. Lipinski, V. Fuster, E. A. Fisher and Z. A. Fayad, *Nat. Clin. Pract. Cardiovasc. Med.,* 2004, **1**, 48-55.

[10] R. P. Choudhury and E. A. Fisher, *Arterioscler. Thromb. Vasc. Biol.,* 2009, **29**, 983-991.

[11] W. J. M. Mulder, D. P. Cormode, S. Hak, M. E. Lobatto, S. Silvera and Z. A. Fayad, *Nat. Clin. Pract. Cardiovasc. Med.* 2008, **5 (Suppl. 2),** S103-S111.

[12] D. P. Cormode, T. Skajaa, Z. A. Fayad and W. J. M. Mulder, *Arterioscler. Thromb. Vasc. Biol.* 2009, **29**, 992-1000.

[13] W. J. M. Mulder, G. J. Strijkers, G. A. F. van Tilborg, D. P. Cormode, Z. A. Fayad and K. Nicolay, *Accounts Chem. Res.*, 2009, **42**, 904-914.

[14] B. Ibañez, J. J. Badimon and M. J. Garcia, *Am. J. Med.* 2009, **122 (Suppl. 1)**, S15-S25.

[15] A. Gallino, M. Stuber, F. Crea, E. Falk, R. Corti, J. Lekakis, J. Schwitter, P. Camici, O. Gaemperli, M. Di Valentino, J. Prior, H. M. Garcia-Garcia, C. Vlachopoulos, F. Cosentino, S. Windecker, G. Pedrazzini, R. Conti, F. Mach, R. De Caterina and P. Libby, 2**012**, *224*, 25-36.

[16] J. Sanz and Z. A. Fayad, *Nature* 2008, **451**, 953-957.

[17] A. J. Sinusas, F. Bengel, M. Nahrendorf, F. H. Epstein, J. C. Wu, F. S. Villanueva, Z. A. Fayad and R. J. Gropler, *Circ. Cardiovasc. Imaging* 2008, **1**, 244-256.

[18] A. Saraste, S. G. Nekolla and M. Schwaiger, *Cardiovasc. Res*. 2009, **83**, 643-652.

[19] M. T. Albelda, E. Garcia-España and J. C. Frias, *Biometals* 2009, **22**, 393-399.

[20] J. C. Frías, M. J. Lipinski, M. T. Albelda, B. Ibáñez, C. Soriano, E. García-España, L. J. Jiménez-Borreguero and J. J. Badimon, *Clin. Med. Cardiol.* 2008, **2**, 173-179.

[21] J. Tang, M. E. Lobatto, J. C. Read, A. J. Mieszawska, Z. A. Fayad and W. J. M. Mulder, *Curr. Cardiovasc. Imaging Rep*., 2012, **5**, 19-25.

[22] Z. A. Fayad, J. T. Fallon, M. Shinnar, S. Wehrli, H. M. Dansky, M. Poon, J. J. Badimon, S. A. Charlton, E. A. Fisher, J. Breslow and V. Fuster, *Circulation* 1998, **98**, 1541-1547.

[23] Z. A. Fayad and V Fuster, *Ann. N. Y. Acad Sci.* 2000, **902**, 173-186.

[24] R. P. Choudhury, V. Fuster, J. J. Badimon, E. A. Fisher and Z. A. Fayad, *Arterioscler. Thromb. Vasc. Biol.* 2002, **22**, 1065-1074.

[25] P. Caravan, J. J. Ellison, T. J. McMurry and R. B. Lauffer, *Chem. Rev.* 1999, **99**, 2293-2352.

[26] C. Corot, P. Robert, J. M. Idée and M. Port, *Adv. Drug Deliver. Rev.* 2006, **58**, 1471-1504.

[27] R. Uppal and P. Caravan, *Future Med. Chem.*, 2010, **2**, 451-470.

[28] B. den Adel, S. M. Bovens, B. te Boekhorst, G. J. Strijkers, R. E. Poelmann, L. van der Weerd and G. Pasterkamp, *Atherosclerosis*, 2012, **225**, 274-280.

[29] *The Chemistry of Contrast Agents in Medical Magnetic Resonance Imaging 2nd Edition*, ed. A. Merbach, L. Helm and E. Toth, John Wiley & Sons, Chichester (England), 2013.

[30] A. Millon, L. Boussel, M. Brevet, J.-L. Mathevet, E. Canet-Soulas, C. Mory, J.-Y. Scoazec and P. Douek, *Stroke*, 2012, **43**, 3023-3028.

[31] L. Boussel, G. Herigault, M. Sigovan, R. Loffroy, E. Canet-Soulas and P. C. Douek, *J. Magn. Reson. Imaging*, 2008, **28**, 533-537.

[32] P. Vakil, J. Vranic, M. C. Hurley, R. A. Bernstein, A. W. Korutz, A. Habib, A. Shaibani, F. H. Dehkordi, T. J. Carroll and S. A. Ansari, *AJNR Am. J. Neuroradiol*., 2013, **34**, 2252-2258.

[33] C. Calcagno, E. Vucic, V. Mani, G. Goldschlager and Z. A. Fayad, *J. Magn. Reson. Imaging*, 2010, **32**, 191-198.

[34] M. E. Gaens, W. H. Backes, S. Rozel, M. Lipperts, S. N. Sanders, K. Jaspers, J. P. M. Cleutjens, J. C. Sluimer, S. Heeneman, M. J. A. P. Daemen, R. J. T. J. Welten, J.-W. H. Daemen, J. E. Wildberger, R. M. Kwee and M. E. Kooi, *Radiology*, 2013, **266**, 271-279.

[35] W. Liu, N. Balu, J. Sun, X. Zhao, H. Chen, C. Yuan, H. Zhao, J. Xu, G. Wang and W. S. Kerwin, *J. Magn. Reson. Imaging*, 2012, **35**, 812-819.

[36] S. S. Virania, D. J. Catellier, L. A. Pompeii, V. Nambi, R. C. Hoogeveen, B. A. Wasserman, J. Coresh, T. H. Mosley, J. D. Otvos, A. R. Sharrett, E. Boerwinkle and C. M. Ballantyne, *Atherosclerosis*, 2011, **219**, 596-602.

[37] J. M. Grimm, K. Nikolaou, A. Schindler, R. Hettich, F. Heigl, C. C. Cyran, F. Schwarz, R. Klingel, A. Karpinska, C. Yuan, M. Dichgans, M. F. Reiser and T. Saam, *J. Cardiovasc. Magn. Reson*., 2012, **14**:80.

[38] G. C. Kane, A. W. Stanson, D. Kalnicka, D. W. Rosenthal, C. U. Lee, S. C. Textor and V. D. Garovic, *Nephrol. Dial Transplant*, 2008, **23**, 1233-1240.

[39] W. S. Kerwin, X. Zhao, C. Yuan, T. S. Hatsukami, K. R. Maravilla, H. R. Underhill and X. Zhao, *J. Magn. Reson. Imaging*, 2009, **30**, 35-40.

[40] C. Brushett, B. Qiu, E. Atalar and X. Yang, *J. Magn. Reson. Imaging*, 2008, **27**, 246-250.

[41] S. Tartari, R. Rizzati, R. Righi, A. Deledda, K. Capello, R. Soverini and G. Benea, *Am. J. Roentgenol*., 2011, **196**, 1164-1171.

[42] W. Chen, E. Vucic, E. Leupold, W. J. M. Mulder, D. P. Cormode, K. C. Briley-Saebo, Alessandra Barazza, E. A. Fisher, M. Dathe and Z. A. Fayad, *Contrast Media Mol. Imaging*, 2008, **3**, 233-242.

[43] V. Amirbekian, M. J. Lipinski, K. C. Briley-Saebo, S. Amirbekian, J. G. S. Aguinaldo, D. B. Weinreb, E. Vucic, J. C. Frias, F. Hyafil, V. Mani, E. A. Fisher and Z. A. Fayad, *Proc. Natl. Acad. Sci. USA*, 2007, **104**, 961-966.

[44] K. C. Briley-Saebo, V. Amirbekian, V. Mani, J. G. S. Aguinaldo, E. Vucic, D. Carpenter, S. Amirbekian and Z. A. Fayad, *Magn. Reson. Med*., 2006, **56**, 1336-1346.

[45] D. Li, A. R. Patel, A. L. Klibanov, C. M. Kramer, M. Ruiz, B.-Y. Kang, J. L. Mehta, G. A. Beller, D. K. Glover and C. H. Meyer, *Circ. Cardiovasc. Imaging*, 2010, **3**, 464-472.

[46] G. A. F. van Tilborg, E. Vucic, G. J. Strijkers, D. P. Cormode, V. Mani, T. Skajaa, C. P. M. Reutelingsperger, Z. A. Fayad, W. J. M. Mulder and K. Nicolay, *Bioconjugate Chem*., 2010, **21**, 1794-1803.

[47] W. Chen, D. P. Cormode, Y. Vengrenyuk, B. Herranz, J. E. Feig, A. Klink, W. J. M. Mulder, E. A. Fisher and Zahi A. Fayad, *J. Am. Coll. Cardiol. Cardiovasc. Imaging*, 2013, **6**, 373-384.

[48] A. N. Lowell, H. Qiao, T. Liu, T. Ishikawa, H. Zhang, S. Oriana, M. Wang, E. Ricciotti, G. A. FitzGerald, R. Zhou and Y. Yamakoshi, *Bioconjugate Chem*., 2012, **23**, 2313-2319.

[49] S. Yasuda, K. Ikuta, T. Uwatoku, K. Oi, K. Abe, F. Hyodo, K. Yoshimitsu, K. Sugimura, H. Utsumi, Y. Katayama and H. Shimokawa, *J. Vasc. Res*., 2008, **45**, 123-128.

[50] S. Laurent, C. Burtea, L. Vander Elst, T. Yamamoto, H. Shimokawa, Y. Katayama and R. N. Muller, *ESMRMB*, 2005, abstract 139.

[51] M. Querol, J. W. Chen, R. Weissleder and A. Bogdanov, Jr., *Org. Lett*., 2005, **7**, 1719-1722.

[52] J. A. Ronald, J. W. Chen, Y. Chen, A. M. Hamilton, E. Rodriguez, F. Reynolds, R. A. Hegele, K. A. Rogers, M. Querol, A. Bogdanov, R. Weissleder and B. K. Rutt, *Circulation*, 2009, **120**, 592-599.

[53] M. J. Lipinski, V. Amirbekian, J. C. Frias, J. G. S. Aguinaldo, V. Mani, K. C. Briley-Saebo, V. Fuster, J. T. Fallon, E. A. Fisher and Z. A. Fayad, *Magn. Reson. Med*., 2006, **56**, 601-610.

[54] K. C. Briley-Saebo, S. Geninatti-Crich, D. P. Cormode, A. Barazza, W. J. M. Mulder, W. Chen, G. B. Giovenzana, E. A. Fisher, S. Aime and Z. A. Fayad, *J. Phys. Chem. B,* 2009**, 113**, 6283–6289.

[55] J. C. Frias, K. J. Williams, E. A. Fisher and Z. A. Fayad, *J. Am. Chem. Soc.* 2004, **126**, 16316–16317.

[56] J. A. Ronald, Y. Chen, A. J.-L. Belisle, A. M. Hamilton, K. A. Rogers, R. A. Hegele, B. Misselwitz and B. K. Rutt, *Circ. Cardiovasc. Imaging*, 2009, **2**, 226-234.

[57] J. Meding, M. Urich, K. Licha, M. Reinhardt, B. Misselwitz, Z. A. Fayad and H.-J. Weinmann, *Contrast Media Mol. Imaging,* 2007, **2**, 120-129.

[58] J. Tanga, Y. Shenga, H. Hub and Y. Shen, *Prog. Polym. Sci*., 2013, **38**, 462-502.

[59] S. Langereis, A. Dirksen, T. M. Hackeng, M. H. P. van Genderen and E. W. Meijer, *New J. Chem*., 2007, **31**, 1152-1160.

[60] C. U. Herborn, M. Schmidt, O. Bruder, E. Nagel, K. Shamsi and J. Barkhausen, *Radiology*, 2004, **233**, 567-573.

[61] P. P. Fatouros, F. D. Corwin, Z. J. Chen, W. C. Broaddus, J. L. Tatum, B. Kettenmann, Z. Ge, H. W. Gibson, J. L. Russ, A. P. Leonard, J. C. Duchamp and H. C. Dorn, *Radiology*, 2006, **240**, 756-764.

[62] Z. Zhou, R. P. Lenk, A. Dellinger, S. R. Wilson, R. Sadler and C. L. Kepley, *Bioconjugate Chem*., 2010, **21**, 1656-1661.

[63] A. Dellinger, J. Olson, K. Link, S. Vance, M. G Sandros, J. Yang, Z. Zhou and C. L. Kepley, *J. Cardiovasc. Magn. Reson*., 2013, **15**:7.

[64] J.-C. Cornily, F. Hyafil, C. Calcagno, K. C. Briley-Saebo, J. Tunstead, J.-G. S. Aguinaldo, V. Mani, V. Lorusso, F. M. Cavagna and Z. A. Fayad, *J. Magn. Reson. Imaging*, 2008, **27**, 1406-1411.

[65] M. R. Makowski, A. J. Wiethoff, U. Blume, F. Cuello, A. Warley, C. H. P. Jansen, E. Nagel, R. Razavi, D. C. Onthank, R. R. Cesati, M. S. Marber, T. Schaeffter, A. Smith, S. P. Robinson and R. M. Botnar, *Nat. Med*., 2011, **17**, 383-388.

[66] M. R. Makowski, S. C. Forbes, U. Blume, A. Warley, C. H. P. Jansen, A. Schuster, A. J. Wiethoff and R. M. Botnar, *Atherosclerosis*, 2012, **222**, 43-49.

[67] K. Overoye-Chan, S. Koerner, R. J. Looby, A. F. Kolodziej, S. G. Zech, Q. Deng, J. M. Chasse, T. J. McMurry and P. Caravan, *J. Am. Chem. Soc*., 2008, **130**, 6025-6039.

[68] F. Hyafil, E. Vucic, J.-C. Cornily, R. Sharma, V. Amirbekian, F. Blackwell, E. Lancelot, C. Corot, V. Fuster, Z. S. Galis, L. J. Feldman and Z. A. Fayad, *Eur. Heart J*., 2011, **32**, 1561-1571.

[69] E. Lancelot, V. Amirbekian, I. Brigger, J.-S. Raynaud, S. Ballet, C. David, O. Rousseaux, S. Le Greneur, M. Port, H. R. Lijnen, P. Bruneval, J.-B. Michel, T. Ouimet, B. Roques, S. Amirbekian, F. Hyafil, E. Vucic, J. G. S. Aguinaldo, C. Corot and Z. A. Fayad, *Arterioscler. Thromb. Vasc. Biol.,* 2008, **28**, 425-432.

[70] H. Alsaid, M. Sabbah, Z. Bendahmane, O. Fokapu, J. Felblinger, C. Desbleds-Mansard, C. Corot, A. Briguet, Y. Crémillieux and E. Canet-Soulas, *Magn. Reson. Med*., 2007, **58**, 1157-1163.

[71] C. Burtea, S. Laurent, O. Murariu, D. Rattat, G. Toubeau, A. Verbruggen, D. Vansthertem, L. Vander Elst and R. N. Muller, *Cardiovasc. Res*., 2008, **78**, 148-157.

[72] C. Burtea, S. Laurent, E. Lancelot, S. Ballet, O. Murariu, O. Rousseaux, M. Port, L. Vander Elst, C. Corot and R. N. Muller, *Mol. Pharm*., 2009, **6**, 1903-1919.

[73] L. Chaabane, N. Pellet, M. C. Bourdillon, C. Desbleds Mansard, A. Sulaiman, G. Hadour, F. Thivolet-Béjui, P. Roy, A. Briguet, P. Douek and E. Canet Soulas, *MAGMA*, 2004, **17**, 188-195.

[74] H. Alsaid, G. De Souza, M.-C. Bourdillon, F. Chaubet, A. Sulaiman, C. Desbleds-Mansard, L. Chaabane, C. Zahir, E. Lancelot, O. Rousseaux, C. Corot, P. Douek, A. Briguet, D. Letourneur and E. Canet-Soulas, *Invest. Radiol*., 2009, **44**, 151-158.

[75] Manuscript in preparation.

[76] E. Gianolio, G. B. Giovenzana, D. Longo, I. Longo, I. Menegotto and S. Aime, *Chem. Eur. J*., 2007, **13**, 5785-5797.

[77] M. Ohgushi, K. Nagayama and A. Wada, *J. Magn. Reson*., 1978, **29**, 599–601.

[78] D. E. Sosnovik, M. Nahrendorf and R. Weissleder, *Basic Res. Cardiol*., 2008, **103**, 122-130.

[79] C. Corot, P. Robert, J.-M. Idée and M. Port, *Adv. Drug Deliv. Rev*., 2006, **58**, 1471-1504.

[80] K. C. Briley-Saebo, V. Mani, F. Hyafil, J.-C. Cornily, and Z. A. Fayad, Magn. Reson. Med., 2008, **59**, 721-730.

[81] S. G. Ruehm, C. Corot, P. Vogt, S. Kolb and J. F. Debatin, *Circulation*, 2001, **103**, 415-422.

[82] Q. Zhou, K.-R. Yang, P. Gao, W.-L. Chen, D.-Y. Yang, M.-J. Liang and L. Zhu, *J. Magn. Reson. Imaging,* 2011, **34**, 1325-1332.

[83] S. A. Schmitz, M. Taupitz, S. Wagner, K.-J. Wolf, D. Beyersdorff and B. Hamm, *J. Magn. Reson. Imaging,* 2001, **14**, 355-361.

[84] M. A. McAteer, J. E. Schneider, Z. A. Ali, N. Warrick, C. A. Bursill, C. von zur Muhlen, D. R. Greaves, S. Neubauer, K. M. Channon and R. P. Choudhury, *Arterioscler. Thromb. Vasc. Biol.*, 2008, **28**, 77-83.

[85] G. Korosoglou, R. G. Weiss, D. A. Kedziorek, P. Walczak, W. D. Gilson, M. Schär, D. E. Sosnovik, D. L. Kraitchman, R. C. Boston, J. W. M. Bulte, R. Weissleder and M. Stuber, *J. Am. Coll. Cardiol.*, 2008, **52**, 483-491.

[86] M. Nahrendorf, F. A. Jaffer, K. A. Kelly, D. E. Sosnovik, E. Aikawa, P. Libby and R. Weissleder, *Circulation*, 2006, **114**, 1504-1511.

[87] T. Y. Tang, K. H. Muller, M. J. Graves, Z. Y. Li, S. R. Walsh, V. Young, U. Sadat, S. P. Howarth and J. H. Gillard, *Arterioscler. Thromb. Vasc. Biol.,* 2009, **29**, 1001-1008.

[88] G. E. Gold, J. M. Pauly, G. H. Glover, J. C. Moretto, A. Moacovki and R. J. Herfkens, *J. Magn. Reson. Imaging,* 1993, **3**, 399-407.

[89] K. C. Briley-Saebo, T. H. Nguyen, A. M. Saeboe, Y.-S. Cho, S. K. Ryu, E. Volkava, S. Dickson, G. Leibundgut, P. Weisner, S. Green, F. Casanada, Y. I. Miller, W. Shaw, J. L. Witztum, Z. A. Fayad and S. Tsimikas, *J. Am. Coll. Cardiol*., 2012, **59**, 616-626.

[90] K. J. Hallock and J. A. Hamilton, *Magn. Reson. Med*., 2006, **56**, 1380-1383.

[91] W. B. Eubank, U. P. Schmiedl, C. Yuan, C. D. Black, K. E. Kellar, D. L. Ladd and J. A. Nelson, *J. Magn. Reson. Imaging*, 1998, **8**, 1051-1059.

[92] H. Zhang, L. Zhang, J. Myerson, K. Bibee, M. Scott, J. Allen, G. Sicard, G. Lanza and S. Wickline, *PLoS One* 2011, **6**, e26385.

[93] L. E. Olsson, C. M. Chai, O. Axelsson, M. Karlsson, K. Golman and J. S. Petersson, *Magn. Reson. Med.* 2006, **55**, 731-737.

[94] P. Bhattacharya, E. Y. Chekmenev, W. F. Reynolds, S. Wagner, N. Zacharias, H. R. Chan, R. Bünger and B. D. Ross, *NMR Biomed*. 2011, **24**, 1023-1028.

[95] K. H. Schuleri, R. T. George and A. C. Lardo, *Nat. Rev. Cardiol*. 2009, **6**, 699-710.

[96] H. Lusic and M. W. Grinstaff, *Chem. Rev*., 2013, **113**, 1641-1666.

[97] J. Ding, Y. Wang, M. Maa, Y. Zhang, S. Lu, Y. Jiang, C. Qi, S. Luo, G. Dong, S. Wen, Y. An and N. Gu, *Biomaterials*, 2013, **34**, 209-216.

[98] R. Bhavane, C. Badea, K. B. Ghaghada, D. Clark, D. Vela, A. Moturu, A. Annapragada, G. A. Johnson, J. T. Willerson and A. Annapragada, *Circ. Cardiovasc. Imaging*, 2013, **6**, 285-294.

[99] D. Danila, R. Partha, D. B. Elrod, M. Lackey, S. W. Casscells and J. L. Conyers, *Tex. Heart Inst. J*., 2009, **36**, 393-403.

[100] A. Schuhbäck, M. Marwan, S. Gauss, G. Muschiol, D. Ropers, C. Schneider, M. Lell, J. Rixe, C. Hamm, W. G. Daniel and S. Achenbach, *Eur. Radiol*., 2012, **22**, 1529-1536.

[101] J. E. van Velzen, J. D. Schuijf, J. M. van Werkhoven, B. A. Herzog, A. P. Pazhenkottil, E. Boersma, F. R. de Graaf, A. J. Scholte, L. J. Kroft, A. de Roos, M. P. Stokkel, J. W. Jukema, P. A. Kaufmann, E. E. van der Wall and J. J. Bax, *Circ. Cardiovasc. Imaging*, 2010, **3**, 718-726.

[102] A. L. Figueroa, S. S. Subramanian, R. C. Cury, Q. A. Truong, J. A. Gardecki, G. J. Tearney, U. Hoffmann, T. J. Brady and A. Tawakol, *Circ. Cardiovasc. Imaging*, 2012, **5**, 69-77.

[103] F. Schwarz, J. W. Nance, B. Ruzsics, G. Bastarrika, A. Sterzik and U. J. Schoepf, *Radiology*, 2012, **264**, 700-707.

[104] K. M. Takakuwa and E. J. Halpern, *Radiology*, 2008, **248**, 438-446.

[105] F. Hyafil, J.-C. Cornily, J. E. Feig, R. Gordon, E. Vucic, V. Amirbekian, E. A. Fisher, V. Fuster, L. J. Feldman and Z. A. Fayad, *Nat. Med*., 2007, **13**, 636-641.

[106] J. F. Hainfeld, D. N. Slatkin, T. M. Focella and H. M. Smilowitz, *Br. J. Radiol.* 2006, **79**, 248-253.

[107] D. P. Cormode, T. Skajaa, M. M. van Schooneveld, R. Koole, P. Jarzyna, M. E. Lobatto, C. Calcagno, A. Barazza, R. E. Gordon, P. Zanzonico, E. A. Fisher, Z. A. Fayad and W. J. Mulder, *Nano Lett.* 2008, **8**, 3715-1723.

[108] G. L. Duff, G. C. McMillan and E. V. Lautsch, *Am. J. Pathol.* 1954, **30**, 941-955.

[109] W. K. Erly, J. Zaetta, G. T. Borders, H. Ozgur, D. R. Gabaeff, R. F. Carmody and J. Seeger, *Am. J. Neuroradiol.* 2000, **21**, 964-967.

[110] H. Hashimoto, S. Hama, K. Yamane and K. Kurisu, *Neurosurg. Rev.*, 2013, **36**, 421-427.

[111] J. S. Meyer, H. Okayasu, H. Tachibana and T. Okabe, *Stroke* 1984, **15**, 80-90.

[112] N. Miyazawa, K. Hashizume, M. Uchida and H. Nukui, *AJNR Am. J. Neuroradiol*. 2001, **22**, 243-247.

[113] L. W. Dobrucki and A. J. Sinusas, *Nat. Rev. Cardiol*. 2010, **7**, 38-47.

[114] O. Schillaci, R. Danieli, F Padovano, A. Testa and G. Simonetti, *Int. J. Mol. Med.* 2008, **22**, 3-7.

[115] K. P. Schäfers and L. Stegger, *Basic Res. Cardiol.* 2008, **103**, 191-199.

[116] S. G. Nekolla, A. Martinez-Moeller and A. Saraste, *Eur. J. Nucl. Med. Mol. Imaging* 2009, **36 (Suppl. 1)**, S121-S130.

[117] T. Temma and H. Saji, *Am. J. Nucl. Med. Mol. Imaging*, 2012, **2**, 432-447.

[118] M. Elkhawad and J. H. F. Rudd, *Cardiol. Clin.* 2009, **27**, 345-354.

[119] L. M. Riou, A. Broisat, J. Dimastromatteo, G. Pons, D. Fagret and C. Ghezzi, *Curr. Med. Chem.* 2009, **16**, 1499-1511.

[120] S. Vemulapalli, S. D. Metzler, G. Akabani, N. A. Petry, N. J. Niehaus, X. Liu, N. H. Patil, K. L. Greer, R. J. Jaszczak, R. E. Coleman, C. Dong, P. J. Goldschmidt-Clermont and B. B. Chin, *Radiology* 2007, **242**, 198-207.

[121] B. L. Kietselaer, C. P. Reutelingsperger, G. A. Heidendal, M. J. Daemen, W. H. Mess, L. Hofstra and J. Narula, *N. Engl. J. Med.* 2004, **350**, 1472-1473.

[122] D. R. Elmaleh, J. Narula, J. W. Babich, A. Petrov, A. J. Fischman, B.-A. Khaw, E. Rapaport and P. C. Zamecnik, *Proc. Natl. Acad. Sci. USA*, 1998, **95**, 691-695.

[123] M. De Saint-Hubert, F. M. Mottaghy, K. Vunckx, J. Nuyts, H. Fonge, K. Prinsen, S. Stroobants, L. Mortelmans, N. Deckers, L. Hofstra, C. P. M. Reutelingsperger, A. Verbruggen and D. Rattat, *Bioorg. Med. Chem*., 2010, **18**, 1356-1363.

[124] M. De Saint-Hubert, M. Bauwens, N. Deckers, M. Drummen, K. Douma, P. Granton, G. Hendrikx, D. Kusters, J. Bucerius, C. P. M. Reutelingsperger and F. M. Mottaghy, *Mol. Imaging Biol*., 2013, doi: 10.1007/s11307-013-0677-0.

[125] H. Morikawi, M. Matsumoto, N. Handa, K. Hahikawa, M. Hori and T. Nishimura, *Nucl. Med. Commun*., 2000, **21**, 1051-1058.

[126] L. L. Johnson, L. Schofield, T. Donahay, N. Narula and J. Narula, *J. Nucl. Med*., 2005, **46**, 1186-1193.

[127] A. M. Lees, R. S. Lees, F. J. Schoen, J. L. Isaacsohn, A. J. Fischman, K. A. McKusick and H. W. Strauss, *Arteriosclerosis*, 1988, **8**, 461-470.

[128] G. Qin, Y. Zhang, W. Cao, R. An, Z. Gao, G. Li, W. Xu, K. Zhang and S. Li, *Eur. J. Nucl. Med. Mol. Imaging*, 2005, **32**, 6-14.

[129] J. E. van Velzen, J. D. Schuijf, J. M. van Werkhoven, B. A. Herzog, A. P. Pazhenkottil, E. Boersma, F. R. de Graaf, A. J. Scholte, L. J. Kroft, A. de Roos, M. P. Stokkel, J. W. Jukema, P. A. Kaufmann, E. E. van der Wall and J. J. Bax, *Circ. Cardiovasc. Imaging*, 2010, **3**, 718-726.

[130] A. Annovazzi, E. Bonanno, M. Arca, C. D'Alessandria, A. Marcoccia, L. G. Spagnoli, F. Violi, F. Scopinaro, G. De Toma and A. Signore, *Eur. J. Nucl. Med. Mol. Imaging*, 2006, **33**, 117-126.

[131] M. Razavian, R. Marfatia, H. Mongue-Din, S. Tavakoli, A. J. Sinusas, J. Zhang, L. Nie and M. M. Sadeghi, *Arterioscler. Thromb. Vasc. Biol*., 2011, **31**, 2820-2826.

[132] S. Tsimikas, W. Palinsid, b S. E. Halpern, D. W. Yeung, L. K. Curtiss and J. L. Witztum**,** *J. Nucl. Cardiol*., 1999, **6**, 41-55.

[133] S. Ohshima, A. Petrov, S Fujimoto, J. Zhou, M. Azure, D. S. Edwards, T. Murohara, N. Narula, S. Tsimikas and J. Narula, *J. Nucl. Med*., 2009, **50**, 612-617.

[134] L. M. Dinkelborg, S. H. Duda, H. Hanke, G. Tepe, C. S. Hilger and W. Semmler, *J. Nucl. Med*., 1998, **39**, 1819-1822.

[135] M. Nahrendorf, E. Keliher, P. Panizzi, H. Zhang, S. Hembrador, J.-L. Figueiredo, E. Aikawa, K. Kelly, P. Libby and R. Weissleder, *J. Am. Coll. Cardiol. Cardiovasc. Imaging,* 2009, **2**, 1213-1222.

[136] J. Zhang, L. Nie, M. Razavian, M. Ahmed, L. W. Dobrucki, A. Asadi, D. S. Edwards, M. Azure, A. J. Sinusas and M. M. Sadeghi, *Circulation*, 2008, **118**, 1953-1960.

[137] R. V. Hay, D. D. Casalino, L. Kordylewski, R. W. Atcher, M. W. Brechbiel, O. A. Gansow, U. Sharokhizadeh, R. M. Fleming, K. A. Lathrop, V. J. Stark and P. V. Harper, *Cardiovasc. Pathol*., 1992, **1**, 189-198.

[138] J. M. U. Silvola, A. Saraste, S. Forsback, V. J. O. Laine, P. Saukko, S. E. Heinonen, S. Ylä-Herttuala, A. Roivainen and J. Knuuti, *Arterioscler. Thromb. Vasc. Biol.,* 2011, **31**, 1011-1015.

[139] C. R. Fischer, A. Müller, B. Bochsler, Z. Rancic, P. Kaufmann, R. Schibli and S. M. Ametamey, *Am. J. Nucl. Med. Mol. Imaging*, 2013, **3**, 326-335.

[140] D. R. Elmaleh, A. J. Fischman, A. Tawakol, A. Zhu, T. M. Shoup, U. Hoffmann, A.-L. Brownell and P. C. Zamecnik, *Proc. Natl. Acad. Sci. USA*, 2006, **103**, 15992-15996.

[141] C. M. Matter, M. T. Wyss, P. Meier, N. Späth, T. von Lukowicz, C. Lohmann, B. Weber, A. Ramirez de Molina, J. C. Lacal, S. M. Ametamey, G. K. von Schulthess, T. F. Lüscher, P. A. Kaufmann and A. Buck, *Arterioscler. Thromb. Vasc. Biol.,* 2006, **26**, 584-589.

[142] J. H. F. Rudd and Z. A. Fayad, *Nat. Clin. Pract. Cardiovasc. Med.* 2008, **5 (Suppl. 2),** S11-S17.

[143] I. Laitinen, A. Saraste, E. Weidl, T. Poethko, A. W. Weber, S. G. Nekolla, P. Leppänen, S. Ylä-Herttuala, G. Hölzlwimmer, A. Walch, I. Esposito, H.-J. Wester, J. Knuuti and M. Schwaiger, *Circ. Cardiovasc. Imaging*, 2009, **2**, 331-338.

[144] M. R. Dweck, M. W. L. Chow, N. V. Joshi, M. C. Williams, C. Jones, A. M. Fletcher, H. Richardson, A. White, G. McKillop, E. J. R. van Beek, N. A. Boon, J. H. F. Rudd and D. E. Newby, *J. Am. Coll. Cardiol*., 2012, **59**, 1539-1548.

[145] J. Hamzah, V. R. Kotamraju, J. W. Seo, L. Agemy, V. Fogal L. M. Mahakian, D. Peters, L. Roth, M. K. J. Gagnon, K. W. Ferrara and E. Ruoslahti, *Proc. Natl. Acad. Sci. USA*, 2011, **108**, 7154-7159.

[146] S. V. Selivanova, T. Stellfeld, T. K. Heinrich, A. Müller, S. D. Krämer, P. A. Schubiger, R. Schibli, S. M. Ametamey, B. Vos, J. Meding, M. Bauser, J. Hütter and L. M. Dinkelborg, *J. Med. Chem*., 2013, **56**, 4912-1920.

[147] A. Broisat, L. M. Riou, V. Ardisson, D. Boturyn, P. Dumy, D. Fagret and C. Ghezzi, *Eur. J. Nucl. Med. Mol. Imaging*, 2007, **34**, 830-840.

[148] C. M. Matter, P. K. Schuler, P. Alessi, P. Meier, R. Ricci, D. Zhang, C. Halin, P. Castellani, L. Zardi, C. K. Hofer, M. Montani, D. Neri and T. F. Lüscher, *Circ. Res.,* 2004, **95**, 1225-1233.

[149] M. Chakrabarti, K. T. Cheng, K. M. Spicer, W. M. Kirsch, S. D. Fowler, W. Kelln, S. Griende, S. Nehlsen-Cannarella, R. Willerson, S. S. Spicer and T. Koch, *Nucl. Med. Biol.,* 1995, **22**, 693-697.

[150] M. Schäfers, B. Riemann, K. Kopka, H.-J. Breyholz, S. Wagner, K. P. Schäfers, M. P. Law, O. Schober and B. Levkau, *Circulation*, 2004, **109**, 2554-2559.

[151] A. Hubalewska–Dydejczyk, T. Stompór, M. Kalembkiewicz, M. Krzanowski, R. Mikolajczak, A. Sowa–Staszczak, B. Tabor–Ciepiela, U. Karczmarczyk, B. Kusnierz–Cabala and W. Sulowicz, *Periton. Dialysis Int*., 2009, **29**, 568-574.

[152] I. Virgolini, F. Rauscha, G. Lupattelli, P. Angelberger, A. Ventura, J. O'Grady and H. Sinzinger, *Eur. J. Nucl. Med*., 1991, **18**, 948-951.

[153] R. Hardoff, F. Braegelmann, P. Zanzonico, E. M. Herrold, R. S. Lees, A. M. Lees, R. T. Dean, J. Lister-James and J. S. Borer, *J. Clin. Pharmacol*., 1993, **33**, 1039-1047.

[154] H. F. Langer, R. Haubner, B. J. Pichler and M. Gawaz, *J. Am. Coll. Cardiol.,* 2008, **52**, 1-12.

[155] W. Xiao, L. Wang, T. Scott, R. E. Counsell and H. Liu, *Pharm. Res*., 1999, **16**, 420-426.

[156] W. Xiao, T. M. Scott, L. Feng, Z. Yu, L. Wang, J. A. Hughes and H. Liu, *J. Nucl. Med*., 2003, **44**, 770-773.

[157] M. Gawaz, I. Konrad, A. I. Hauser, S. Sauer, Z. Li, H.-J. Wester, F. M. Bengel, M. Schwaiger, A. Schömig, S. Massberg and R. Haubner, *Thromb. Haemost*., 2005, **93**, 910-913.

[158] P. X. Shaw, S. Hörkkö, S. Tsimikas, M.-K. Chang, W. Palinski, G. J. Silverman, P. P. Chen and J. L. Witztum, *Arterioscler. Thromb. Vasc. Biol*., 2001, **21**, 1333-1339.

[159] L. Iuliano, A. Mauriello, E. Sbarigia, L. G. Spagnoli and F. Violi, *Circulation*, 2000, **101**, 1249-1254.

[160] M. Torzewski, P. X. Shaw, K.-R. Han, B. Shortal, K. J. Lackner, J. L. Witztum, W. Palinski and S. Tsimikas, *Arterioscler. Thromb. Vasc. Biol*., 2004, **24**, 2307-2312.

[161] K. Nishigori, T. Temma, K. Yoda, S. Onoe, N. Kondo, M. Shiomi, M. Ono and H. Saji, *Nucl. Med. Biol*., 2013, **40**, 97-103.

[162] P. Lu, P. Zanzonico, J. Lister-James, S. M. Goldfine, E. Herrold, R. S. Lees, A. M. Lees, R. T. Dean, B. R. Moyer and J. S. Borer, *Am. J. Ther*., 1996, **3**, 673-680.

[163] A. Rominger, T. Saam, E. Vogl, C. Ubleis, C. la Fougère, S. Förster, A. Haug, P. Cumming, M. F. Reiser, K. Nikolaou, P. Bartenstein and M. Hacker, *J. Nucl. Med*. 2010, **51**, 193-197.

[164] C. Xu, F. Li, G. Niu and X. Chen, *Theranostics*, 2013, **3**, 448-466.

[165] J. Haukkala, I. Laitinen, P. Luoto, P. Iveson, I. Wilson, H. Karlsen, A. Cuthbertson, J. Laine, P. Leppänen, S. Ylä-Herttula, J. Knuuti and A. Roivainen, *Eur. J. Nucl. Med. Mol. Imaging*, 2009, **36**, 2058-2067.

[166] Y. Liu, D. Abendschein, G. E. Woodard, R. Rossin, K. McCommis, J. Zheng, M. J. Welch and P. K. Woodard, *J. Nucl. Med*., 2010, **51**, 85-91.

[167] B. R. Jarrett, C. Correa, K. L. Ma and A. Y. Louie, *PLos ONE*, 2010, **5**, e13254.

[168] M. Nahrendorf, H. Zhang, S. Hembrador, P. Panizzi, D. E. Sosnovik, E. Aikawa, P. Libby, F. K. Swirski and R. Weissleder, *Circulation*, 2008, **117**, 379-387.

[169] M. D. Majmudar, J. Yoo, E. J. Keliher, J. J. Truelove, Y. Iwamoto, B. Sena, P. Dutta, A. Borodovsky, K. Fitzgerald, M. F. Di Carli, P. Libby, D. G. Anderson, F. K. Swirski, R. Weissleder and M. Nahrendorf, *Circ. Res*., 2013, **122**, 755-761.

[170] R. Golestani, C. J. Zeebregts, A. G. T. T. van Scheltinga, M. N. Lub-de Hooge, G. M. van Dam, A. W. J. M. Glaudemans, R. A. J. O. Dierckx, R. A. Tio, A. J. H. Suurmeijer, H. H. Boersma, W. B. Nagengast and R. H. J. A. Slart, *Mol. Imaging*, 2013, **12**, 235-243.

[171] *Molecular Imaging, Radiopharmaceuticals for PET and SPECT*, ed. S. Vallabhjosula, Springer, 2009.

[172] T. Derlin, C. R. Habermann, Z. Lengyel, J. D. Busch, C. Wisotzki, J. Mester and L. Pávics, *J. Nucl. Med*., 2011, **52**, 1848-1854.

[173] K. Kato, O. Schober, M. Ikeda, M. Schäfers, T. Ishigaki, P. Kies, S. Naganawa and L. Stegger, *Eur. J. Nucl. Med. Mol. Imaging*, 2009, **36**, 1622-1628.

[174] O. Gaemperli, J. Shalhoub, D. R. J. Owen, F. Lamare, S. Johansson, N. Fouladi, A. H. Davies, O. E. Rimoldi and P. G. Camici, *Eur. Heart J*., 2012, **33**, 1902-1910.

[175] H. Tsutsui, H. Tomoike and M. Nakamura, *Circ. Res*., 1990, **67**, 368-375.

[176] J. L. E. Bird, D. Izquierdo-Garcia, J. R. Davies, J. H. F. Rudd, K. C. Probst, N. Figg, J. C. Clark, P. L. Weissberg, A. P. Davenport and E. A. Warburton, Atherosclerosis, 2010, **210**, 388-391.

[177] J. R. Lindner, *Nat. Rev. Drug. Discov.* 2004, **3**, 527-532.

[178] J. R. Lindner, *Nat. Rev. Cardiol.* 2009, **6**, 475-481.

[179] H. Liu, X. Wang, K.-B. Tan, P. Liu, Z.-X. Zhuo, Z. Liu, X. Hua, Q.-Q. Zhuo, H.-M. Xia and Y.-H. Gao, *J. Clin. Ultrasound*, 2011, **39**, 83-90.

[180] B. A. Kaufmann, J. M. Sanders, C. Davis, A. Xie, P. Aldred, I. J. Sarembock and J. R, Lindner, *Circulation* 2007, **116**, 276-284.

[181] S. C. H. van den Oord, G. L. ten Kate, E. J. G. Sijbrands, A. F. W. van der Steen and A. F. L. Schinkel, *Am. J. Cardiol*., 2013, **111**, 754-759.

[182] E. C. Unger, P. J. Lund, D. K. Shen, T. A. Fritz, D. Yellowhair and T. E. New, *Radiology*, 1992, **185**, 453-456.

[183] S. M. Demos, H. Alkan-Onyuksel, B. J. Kane, K. Ramani, A. Nagaraj, R. Greene, M. Klegerman and D. D. McPherson, *J. Am. Coll. Cardiol*., 1999, **33**, 867-875.

[184] A. Wunder and J. Klohs, *Basic Res. Cardiol*., 2008, **103**, 182-190.

[185] J. Klohs, A. Wunder and K. Licha, *Basic Res. Cardiol*., 2008, **103**, 144-151.

[186] K. Park , H.-Y. Hong, H. J. Moon, B.-H. Lee, I.-S. Kim, I. C. Kwon and K. Rhee, *J. Control Release*, 2008, **128**, 217-223.

[187] M. Nahrendorf, P. Waterman, G. Thurber, K. Groves, M. Rajopadhye, P. Panizzi, B. Marinelli, E. Aikawa, M. J. Pittet, F. K. Swirski and R. Weissleder, *Arterioscler. Thromb. Vasc. Biol.,* 2009, **29**, 1444-1451.

[188] C. Buono, J. J. Anzinger, M. Amar and H. S. Kruth, *J. Clin. Invest*., 2009, **119**, 1371-1381.

[189] B. den Adel, S. M. Bovens, B. te Boekhorst, G. J. Strijkers, R. E. Poelmann, L. van der Weerd and G. Pasterkamp, *Atherosclerosis*, 2012, **225**, 274-280.

[190] F. A. Jaffer, D.-E. Kim, L. Quinti, C.-H. Tung, E. Aikawa, A. N. Pande, R. H. Kohler, G.-P. Shi, P. Libby and R. Weissleder, *Circulation*, 2007, **115**, 2292-2298.

[191] V. Neave, S. Giannotta, S. Hyman and J. Schenider, *Neurosurgery*, 1988, **23**, 307-312.

[192] B. A. Kaufmann, J. M. Sanders, C. Davis, A Xie, P. Aldred, I. J. Sarembock and J. R. Lindner, *Arterioscler. Thromb. Vasc. Biol*. 2010, **30**, 54-59.

[193] A. Jayagopal, Y. R. Su, J. L. Blakemore, M. F. Linton, S. Fazio and F. R. Haselton, *Nanotechnology*, 2009, **20**, 165102.

[194] T. M. Chou, K. W. Woodburn, W. F. Cheong, S. A. Lacy, K. Sudhir, D. C. Adelman and D. Wahr, *Catheter. Cardio. Inte.,* 2002, **57**, 387-394.

[195] V. Amirbekian, J. G. S. Aguinaldo, S. Amirbekian, F. Hyafil, E. Vucic, M. Sirol, D. B. Weinreb, S. Le Greneur, E. Lancelot, C. Corot, E. A. Fisher, Z. S. Galis and Z. A. Fayad, *Radiology*, 2009, **251**, 429-438.

[196] B. Wang, E. Yantsen, T. Larson, A. B. Karpiouk, S. Sethuraman, J. L. Su, K. Sokolov and S. Y. Emelianov, *Nano Lett.* 2009, **9**, 2212-2217.

[197] M. E. Lobatto, Z. A. Fayad, S. Silvera, E. Vucic, C. Calcagno, V. Mani, S. D. Dickson, K. Nicolay, M. Banciu, R. M. Schiffelers, J. M. Metselaar, L. van Bloois, H.-S. Wu, J. T. Fallon, J. H. Rudd, V. Fuster, E. A. Fisher, G. Storm and W. J. M. Mulder, *Mol. Pharm*., 2010, **7**, 2020-2029.

[198] Y. Uchida, Y. Maezawa, Y. Uchida, N. Hiruta and E. Shimoyama, *PLoS ONE*, 2012, **7**, e50678.

[199] J. M. Criscione, L. W. Dobrucki, Z. W. Zhuang, X. Papademetris, M. Simons, A. J. Sinusas and T. M. Fahmy, *Bioconjugate Chem*., 2011, **22**, 1784-1792.

[200] M. D. Bartholomä, A. S. Louie, J. F. Valliant and J. Zubieta, *Chem. Rev*., 2010, **110**, 2903-2920.

[201] V. C. Pierre, M. J. Allen and P. Caravan, *J. Biol. Inorg. Chem*., 2014, doi: 10.1007/s00775-013-1074-5 and referentes therein.

[202] T. J. Wadas, E. H. Wong, G. R. Weisman and C. J. Anderson, *Chem. Soc. Rev.* 2010, **110**, 2858–2902.

[203] M. D. Bartholomä, A. S. Louie, J. F. Valliant and J. Zubieta, *Chem. Rev*., 2010, **110**, 2903-2920.

[204] V. P. Torchilin, *Nat. Rev. Drug Discov*., 2005, **4**, 145-160.

[205] D. Pan, S. D. Caruthers, J. Chen, P. M. Winter, A. Senpan, A. H. Schmieder, S. A. Wickline and G. M. Lanza, *Future Med. Chem*. 2010, **2**, 471-490.

[206] D. Pan, E. Roessl, J. P. Schlomka, S. D. Caruthers, A. Senpan, M. J. Scott, J. S. Allen, H. Zhang, G. Hu, P. J. Gaffney, E. T. Choi, V. Rasche, S. A. Wickline, R. Proksa and G. M. Lanza, *Angew. Chem. Int. Ed. Engl*. 2010, **49**, 9635-9639.

Table of Contents

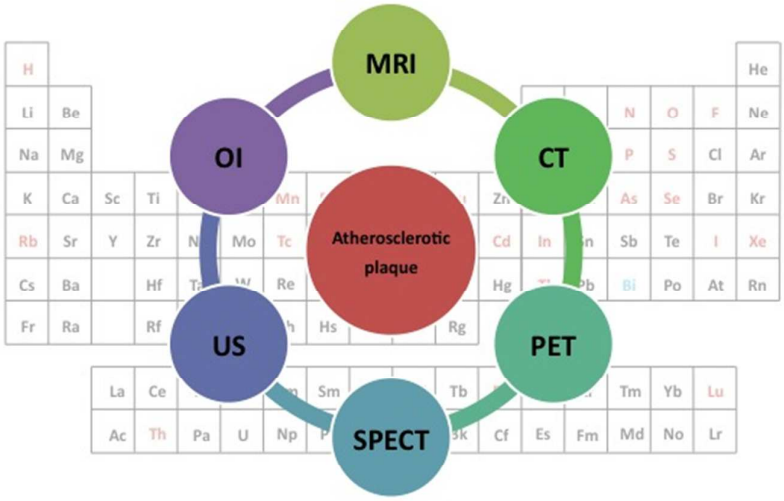

Graphical Abstract

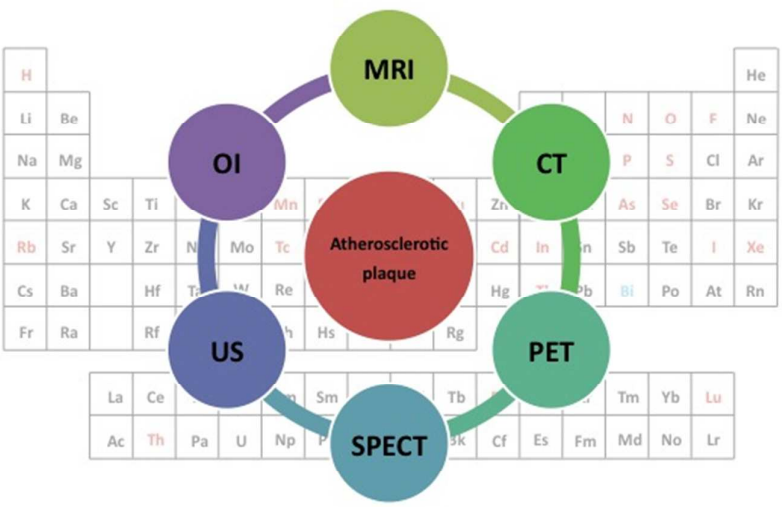

Compounds and imaging techniques used to visualize atherosclerotic plaque, one of the major pathologies causing coronary artery diseases, are discussed.